

CHARACTERIZATION OF YELLOW RUST AND STEM RUST RESISTANT
AND SENSITIVE DURUM WHEAT LINES AT MOLECULAR LEVEL BY
USING BIOPHYSICAL METHODS

A THESIS SUBMITTED TO
THE GRADUATE SCHOOL OF NATURAL AND APPLIED SCIENCES
OF
MIDDLE EAST TECHNICAL UNIVERSITY

BY

ÇİĞDEM KANSU

IN PARTIAL FULFILLMENT OF THE REQUIREMENTS
FOR
THE DEGREE OF MASTER OF SCIENCE
IN
BIOLOGY

SEPTEMBER 2011

Approval of the Thesis:

**CHARACTERIZATION OF YELLOW RUST AND STEM RUST
RESISTANT AND SENSITIVE DURUM WHEAT LINES AT MOLECULAR
LEVEL BY USING BIOPHYSICAL METHODS**

submitted by **ÇİĞDEM KANSU** in partial fulfillment of the requirements for the degree of **Master of Science in Department of Biology, Middle East Technical University** by,

Prof. Dr. Canan Özgen _____
Dean, **Graduate School of Natural and Applied Sciences**

Prof. Dr. Musa Doğan _____
Head of the Department, **Biology, METU**

Prof. Dr. Zeki Kaya _____
Supervisor, **Biology Department, METU**

Prof. Dr. Feride Severcan _____
Co-Supervisor, **Biology Department, METU**

Examining Committee Members:

Prof.Dr. Gülsün Gökağaç _____
Chemistry Department, METU

Prof. Dr. Zeki Kaya _____
Biology Department, METU

Assoc. Prof. Sertaç Önde _____
Biology Department, METU

Assoc. Prof. Ayşegül Gözen _____
Biology Department, METU

Assis. Prof. Sevgi Türker _____
Biology Department, Kocaeli University

Date: 09.09.2011

I hereby declare that all information in this document has been obtained and presented in accordance with academic rules and ethical conduct. I also declare that, as required by these rules and conduct, I have fully cited and referenced all material and results that are not original to this work.

Name-Surname: iđdem Kansu

Signature :

ABSTRACT

CHARACTERIZATION OF YELLOW RUST AND STEM RUST RESISTANT AND SENSITIVE DURUM WHEAT LINES AT MOLECULAR LEVEL BY USING BIOPHYSICAL METHODS

Kansu, iğdem

M. Sc. Department of Biology

Supervisor: Prof. Dr. Zeki Kaya

Co-Supervisor: Prof. Dr. Feride Severcan

September, 2011, 90 pages

Stem rust and Yellow rust diseases are the two major wheat fungal diseases causing considerable yield losses in Turkey and all around the world. There are studies which are carried out to identify and utilize resistance sources in order to obtain resistant lines of wheat. However, virulent pathotypes are continuously being important threats to wheat production and yield. For that reason, new approaches for rapid identification are needed.

The aim of this study was to investigate and to understand the structural and functional differences between the resistant and sensitive durum wheat cultivars to the plant fungal diseases of stem and yellow (stripe) rusts. To aim this, forty durum wheat recombinant inbred lines (RILs), which were previously determined to be resistant or sensitive to stem and yellow rust diseases, were investigated by the non-invasive Attenuated Total Reflectance Fourier Transform Infrared (ATR-FTIR) Spectroscopy. Also, classification of the resistant and sensitive lines depending on the structural and functional differences has been attempted.

The FTIR spectra for stem rust disease showed that, resistant durum wheat lines had a significant increase in the population of unsaturation in acyl chains of lipid molecules, an increase in lipid and in total protein content and also an increase in carboxylic acids and alcohols. For yellow rust disease, resistant lines had a significant increase in hydrogen bonding and they had also a more ordered membrane structure.

In Principal Component Analysis for stem rust disease, according to 3700-650 cm^{-1} region, amide III band (1213-1273 cm^{-1} region) and C-H stretching region (3020-2800 cm^{-1}), the resistant and sensitive groups were separated successfully. For yellow rust disease, according to 3700-650 cm^{-1} region, Amide A and Amide III bands, the resistant and sensitive lines were grouped distinctly.

FTIR spectroscopy provides a useful approach to determine the differences in molecular structure of durum wheat RILs regarding resistance of lines to fungal diseases. However, further research is still needed to ensure if the structural and functional differences in biomolecules of the samples could be used as molecular markers for discrimination of rust resistant materials from rust sensitive ones.

Keywords: ATR-FTIR spectroscopy, stem rust, yellow rust, rust disease resistance, Durum wheat, Recombinant inbred lines, characterization

ÖZ

KARA PAS VE SARI PAS HASTALIKLARINA DAYANIKLI VE HASSAS DURUM BUĞDAY HATLARININ MOLEKÜLER DÜZEYDE BİYOFİZİKSEL METODLARLA KARAKTERİZASYONU

Kansu, Çiğdem

Yüksek Lisans, Biyoloji Bölümü

Tez Yöneticisi: Prof. Dr. Zeki Kaya

Ortak Tez Yöneticisi: Prof. Dr. Feride Severcan

Eylül, 2011, 90 sayfa

Kara pas ve Sarı Pas Türkiye’de ve dünyada önemli ölçüde verim kaybına neden olan başlıca buğday mantar hastalıklarıdır. Bu yıkıcı mantar hastalıklarına karşı dayanıklı buğday hatlarının tanımlanması ve bu dayanıklı kaynaklardan yararlanılması için araştırmalar yapılmaktadır. Fakat virulan patotipler buğday üretimi ve verime önemli ölçüde tehdit oluşturmaya devam etmektedir. Bu sebeple, hızlı teşhis için yeni yaklaşımlara ihtiyaç vardır.

Bu çalışmanın amacı bitki mantar hastalıkları kara pas ve sarı pasa karşı dayanıklı ve hassas durum buğday kültürlerinin yapısal ve fonksiyonel farklılıklarını incelemek ve anlamaktır. Bu amaçla, daha önceki çalışmalarda kara pas ve sarı pas hastalıklarına dayanıklı ve hassas olduğu belirlenmiş olan kırk saf durum buğday hattı örneğe zarar vermeyen ATR-FTIR spektroskopisi ile incelendi. Aynı zamanda, bu farklılıklara göre dayanıklı ve hassas hatların sınıflandırılmasının yapılması amaçlandı.

Kara pas FTIR spektrumları, dayanıklı hatların lipid doymamış asil zinciri popülasyonunda, total protein ve total lipid miktarında ve aynı zamanda karboksilik

asit ve alkol miktarında önemli bir artım olduğunu göstermiştir. Sarı pas hastalığı için, dayanıklı hatlar hidrojen bağlarında önemli bir artıma ve daha düzenli bir membran yapısına sahiptir.

Principal Component Analizi kara pas hastalığı için 3700-650 cm^{-1} bölgesi, amid III bandı (1213-1273 cm^{-1} region) ve C-H gerilme bölgesine (3020-2800 cm^{-1}) göre dayanıklı ve hassas grupları başarıyla ayırmıştır. Sarı pas hastalığı için, 3700-650 cm^{-1} bölgesi, Amid A ve Amid III bandlarına göre dayanıklı ve hassas hatlar belirgin bir şekilde gruplanmıştır.

FTIR spektroskopisi durum buğdayı saf hatlarının moleküler yapısındaki farklılıkları belirlemek için yararlı bir yaklaşım sağlamaktadır. Ancak, bu yapısal ve fonksiyonel değişikliklerin dayanıklı bireylerin hassas olanlardan ayrılmasında moleküler belirteç olarak kullanılabilmesini doğrulayan daha fazla araştırma gereklidir.

Anahtar Kelimeler: ATR-FTIR spektroskopisi, kara pas, sarı pas, pas hastalığına dayanıklılık durum buğdayı, Rekombinant kendilenmiş hatlar, karakterizasyon.

To my beloved mom,

ACKNOWLEDGEMENTS

I would like to express my deepest gratitude to my supervisor Prof. Dr. Zeki Kaya and my co-supervisor Prof. Dr. Feride Severcan for their guidance, encouragements and advice throughout the research. I would also like to express my regards to Assoc. Prof. Sertaç Önde for his support and guidance all through my thesis study.

I express my sincere appreciation to all members of thesis examining committee for their comments and criticism.

I would like to thank Nihal Şimşek Özer, Özlem Bozkurt and Sevgi Türker, who helped me with their broad knowledge about the topic.

I am thankful to all my lab partners for their friendship and help. I also compassionately express my special thanks to Ayten Dizkırıcı and Evrim Zeybek owing to their precious help and lovely attitude in writing this thesis and for their guidance, support and encouragements all through my life.

Finally, I would like to express my deepest thanks to my father and brother for their love, patience, insight, support and encouragements. I would also like to express my special thanks to my love, Tuna for his endless support and patience.

TABLE OF CONTENTS

ABSTRACT	iv
ÖZ	vi
ACKNOWLEDGEMENTS	ix
TABLE OF CONTENTS	x
LIST OF TABLES	xiii
LIST OF FIGURES	xiv
LIST OF ABBREVIATIONS	xvii
CHAPTERS	
1.INTRODUCTION	1
1.1. Wheat.....	1
1.1.1. Taxonomy	1
1.1.2. Wheat production in world and Turkey	1
1.1.3. Durum Wheat.....	3
1.1.4. Wheat Rust Diseases.....	6
1.1.4.1. Stem Rust	7
1.1.4.1.1. Life cycle of Stem Rust & Infection Process	8
1.1.4.1.2. Stem Rust Epidemics in Turkey & in the World.....	10
1.1.4.1.3. Genetic Resistance to Stem Rust.....	11
1.1.4.2. Yellow rust (Stripe Rust)	12
1.1.4.2.1. Life cycle of Yellow rust & Infection Process	13
1.1.4.2.2. Yellow rust Epidemics	15

1.1.4.2.3. Genetic Resistance to Yellow rust.....	17
1.1.4.3. Breeding Wheat for Rust Disease Resistance	19
1.2. Spectroscopy	21
1.2.1. Electromagnetic Radiation and Optical Spectroscopy.....	21
1.2.2. Basis of Infrared Spectroscopy	25
1.2.2.1. Fourier Transform Infrared Spectroscopy (FTIR)	27
1.2.2.2. The Advantages of FTIR Spectroscopy	29
1.2.2.3. Attenuated Total Reflectance (ATR) FTIR Spectroscopy	30
1.2.2.4. The Use of FTIR Spectroscopy in Plant Classification and Identification	32
1.3. Objective & Justification of the study	34
2.MATERIALS AND METHODS	36
2.1. Plant materials, assessments of yellow and stem rusts	36
2.2. Sample Selection & Preparation for ATR-FTIR spectroscopy	38
2.3. ATR-FTIR spectroscopy.....	38
2.4. Statistical Analysis.....	39
2.5. Principal Component Analysis (PCA)	39
3.RESULTS	40
3.1. General FTIR Spectra and Band Assignment of Durum Wheat RIL Seeds ...	40
3.2. Comparison of Stem Rust Resistant and Sensitive Durum Wheat Lines.....	44
3.2.1. Numerical Comparisons of the Bands of Stem Rust Resistant and Sensitive Durum Wheat Lines	50
3.2.2. Detailed Spectral Analysis.....	53
3.2.2.1. Comparison of Stem Rust Resistant and Sensitive Spectra in 3700- 2800 cm ⁻¹ Region	53
3.2.2.2. Comparison of Stem Rust Resistant and Sensitive Spectra in 1800-650 cm ⁻¹ Region	55
3.3. Comparison of Yellow (Stripe) Rust Resistant and Sensitive Durum Wheat Lines	57

3.3.1. Numerical Comparisons of the Bands of Yellow Rust Resistant and Sensitive Durum Wheat Lines	61
3.3.2. Detailed Spectral Analysis.....	64
3.3.2.1. Comparison of Yellow Rust Resistant and Sensitive Spectra in 3700-2800 cm ⁻¹ Region	64
3.3.2.2. Comparison of Yellow Rust Resistant and Sensitive Spectra in 1800-650 cm ⁻¹ Region	65
4.DISCUSSION	68
4.1. Discussion on Resistant and Sensitive RILs to Stem Rust Disease	68
4.2. Discussion on Resistant and Sensitive RILs to Yellow Rust Disease.....	70
5.CONCLUSION.....	72
REFERENCES.....	74

LIST OF TABLES

TABLES

Table 1. Wheat production in the World in million tons.	2
Table 2. Development of 150 lines of F6 progeny of Kunduru-1149_Cham-1cross .	37
Table 3. General band assignment of FT-IR spectrum of plants based on literature	43
Table 4. Numerical summary of the detailed differences in the band frequencies of resistant and sensitive spectra.	51
Table 5. Numerical summary of the detailed differences in the band areas of resistant and sensitive spectra.	52
Table 6. Numerical summary of the detailed differences in the lipid-to-protein ratios of stem rust resistant and sensitive spectra.	55
Table 7. Numerical summary of the detailed differences in the band frequencies of resistant and sensitive spectra.	62
Table 8. Numerical summary of the detailed differences in the band areas of resistant and sensitive spectra.	63
Table 9. Numerical summary of the detailed differences in the lipid-to-protein ratios of yellow rust resistant and sensitive spectra.	65

LIST OF FIGURES

FIGURES

Figure 1. Wheat production in Turkey between 2005 and 2009.....	3
Figure 2. Global Durum Wheat Production between 2002 and 2011.....	4
Figure 3: Durum Wheat Growing Areas.....	5
Figure 5. Life cycle of stem rust <i>Puccinia graminis</i> ssp. <i>tritici</i>	9
Figure 7. Relative resistances of wheat to yellow rust.....	13
Figure 8. Life cycle of stem rust <i>Puccinia striiformis</i> f. sp. <i>tritici</i>	15
Figure 9. The gradual spread of the Yr9-virulent wheat yellow rust from eastern Africa to the South Asia.....	16
Figure 10. Years of the first recorded appearance of the <i>Puccinia striiformis</i> virulence for 8156 cultivars and its possible migration path.....	17
Figure 11. An electromagnetic wave.....	22
Figure 12. Typical energy-level diagrams showing the ground state and the first excited state.....	23
Figure 13. The Electromagnetic spectrum.....	25
Figure 14. The schematic representation of some molecular vibrations in linear triatomic molecules and non-linear triatomic molecules.....	27
Figure 15. Basic components of FTIR spectroscopy.....	28
Figure 16. A multiple reflection ATR system.....	31
Figure 17. The representative infrared spectra of resistant and sensitive groups of stem rust disease in the region between 4000-650cm ⁻¹	41
Figure 19. The representative infrared spectra of resistant and sensitive groups of stem rust disease in the region between 3700- 3000 cm ⁻¹	45
Figure 20. The representative infrared spectra of resistant and sensitive groups of stem rust disease in the region between 3020-2800 cm ⁻¹	45
Figure 21. The representative infrared spectra of resistant and sensitive groups of stem rust disease in the region between 1800-650 cm ⁻¹	46

Figure 22. Classification of Resistant and Sensitive Lines to Stem Rust using PCA based on FTIR spectra.....	47
Figure 23. The representative infrared spectra of resistant and sensitive groups of yellow rust disease in the region between 3700- 3000 cm^{-1}	58
Figure 24. The representative infrared spectra of resistant and sensitive groups of yellow rust disease in the region between 3020-2800 cm^{-1}	58
Figure 25. The representative infrared spectra of resistant and sensitive groups of yellow rust disease in the region between 1800-650 cm^{-1}	59
Figure 26. Classification of Resistant and Sensitive Lines to Yellow Rust using PCA based on FTIR spectra.....	60

LIST OF ABBREVIATIONS

ATR-FTIR	Attenuated Total Reflectance Fourier Transform Infrared Spectroscopy
PCA	Principal Component Analysis
APR	Adult Plant Resistance
R genes	Resistance genes
ITs	Infection types
HTAP	High Temperature Adult Plant Resistance
QTL	Quantitative trait loci
IR	Infrared
KBr	Potassium bromide
RIL	Recombinant inbred line
FTIR	Fourier Transform Infrared
SD	Standard Deviation
R	Resistant
MR	Moderately resistant
MS	Moderately Sensitive
S	Sensitive
DON	Deoxynivalenol
NIR	Near-infrared
ICARDA	International Center for Agricultural Research in the Dry Areas

CHAPTER 1

INTRODUCTION

1.1. Wheat

1.1.1. Taxonomy

Wheat is one of the most widely grown cereal crop together with rice, barley and maize. Wheat provides much of the calories and proteins for our daily life like other cereals rice and maize. It is a member of the Grass family *Gramineae* (*Poaceae*) and the tribe *Triticeae* (*Hordeae*). There are 14 recognized species of *Triticum* genus. The species are classified according to their chromosome copy number and divided into three subgroups; diploid, tetraploid and hexaploid.

1.1.2. Wheat production in world and Turkey

Wheat accounts for around 30% of global grain production and 44% of cereal production, which are used as food. From this production 18% is traded internationally (FAOSTAT, 2009). Globally, around 220 million hectares of land is used for 600 million tons wheat production each year (FAOSTAT, 2009), with nearly half of this area and production attributed to developing countries (Singh & Trethowan, 2007).

The Near East, East and North Africa and Central and South Asia account for 37 percent of global wheat production alone. The world wheat production by March 2011 is approximately 647.597.000metric-tons. As seen in Table 1, according to the recent data obtained from USDA, Turkey is one of the top producers of wheat. (<ftp://ftp.fao.org/docrep/fao/011/i0378e/i0378e.pdf>).

Table 1. Wheat production in the World in million tons (USDA, 2011).

<http://www.fas.usda.gov/psdonline/psdReport.aspx?hidReportRetrievalName=World+Wheat+Production%2c+Consumption%2c+and+Stocks++++++++&hidReportRetrievalID=750&hidReportRetrievalTemplateID=7>, Retrieved on 10/09/2011

Countries-Year	2006/07	2007/08	2008/09	2009/10	2010/11March
EU-27	124,870	120,133	151,122	138,051	136,078
China	108,466	109,298	112,464	115,120	114,500
India	69,350	75,810	78,570	80,680	80,800
Russia	44,900	49,400	63,700	61,700	41,500
Pakistan	21,277	23,295	20,959	24,033	23,900
Canada	25,265	20,054	28,611	26,848	23,167
USA	49,217	55,821	68,016	60,366	60,103
Turkey	17,500	15,500	16,800	18,450	17,000
Argentina	16,300	18,600	11,000	11,000	15,000
Australia	10,822	13,569	21,420	21,923	26,000
Brazil	2,234	3,825	5,880	5,026	5,900
Iran	14,500	15,000	10,000	12,000	14,400
Ukraine	14,000	13,900	25,900	20,900	16,850
World Total	596,115	611,202	684,155	682,594	647,597

In Turkey, like other cereal countries the importance of wheat in human diet is obvious. Wheat is grown annually in the Southeastern Anatolia, Central Anatolia, Mediterranean and Eastern Anatolia regions of Turkey. The wheat production in Turkey is shown in Figure 1 year by year. In 2009, the production area was grown approximately 8.097.898 hectares and production reached at 20.600.000 tons. Durum wheat (*Triticum durum* Desf.), which is a tetraploid wheat species, was used in this study.

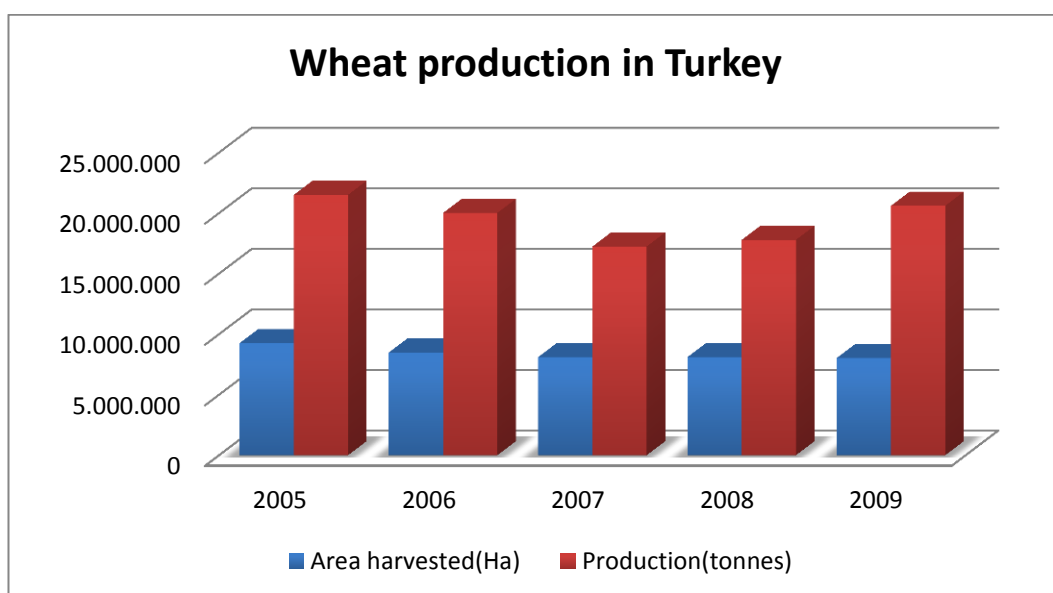


Figure 1. Wheat production in Turkey between 2005 and 2009

(<http://faostat.fao.org/site/567/DesktopDefault.aspx?PageID=567#ancor>). Retrieved on 01/09/2011

1.1.3. Durum Wheat

Durum wheat (*Triticum turgidum* ssp. *durum* or *Triticum durum* Desf.) is a species that belongs to the tribe *Triticeae* and to the genus *Triticum*. It is one of the most important wheat species after the common bread wheat (*Triticum aestivum* L.). It is an allotetraploid species (genome AABB) with 28 chromosomes ($2n=4x=28$). The species lacks D genome found in hexaploid common wheats. The A and B genome donor of durum wheat is wild emmer wheat, *Triticum dicoccoides* (*Triticum turgidum* ssp. *dicoccoides*) (Kimber & Feldman, 1987).

Durum wheat is an important crop for human consumption. It possesses a unique quality that differentiates it from other species. It has the hardest kernel among all wheat species. With its high protein content and its gluten strength, it is the major

wheat species preferred for pasta making. It is used to make semolina, which is used in pasta products such as pasta, bulgur and couscous. It is mainly grown in the Mediterranean region, Canada, the USA, Argentina and India in the world and has the traits such as resistance to diseases (Beharav *et al.*, 1997), environmental stability (Blum *et al.*, 1989; Almansouri *et al.*, 2001), yield potential and high quality (Desai & Bhatia, 1978). In Figure 2, world durum wheat production and yield according to USDA were provided for last seven years (<http://www.pecad.fas.usda.gov/highlights/2010/11/global%20durum/>)

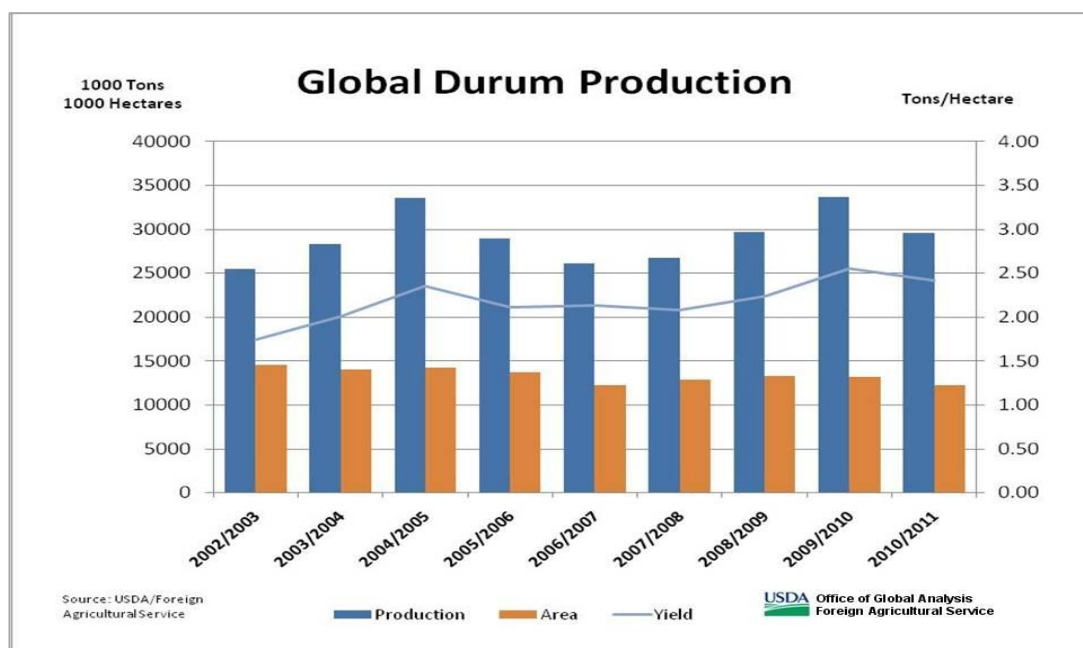


Figure 2. Global Durum Wheat Production between 2002 and 2011.

In Turkey, durum wheat is a traditionally important crop. It is grown in two major regions of Turkey that is the central plateau and transitional zones, and the South Eastern Anatolia.

The Southeastern Anatolia region production comprises about %50-60 of the total durum and the remaining production is in Central Anatolia (Figure 3). Durum wheat constitutes 12 % of total wheat production area in Turkey.

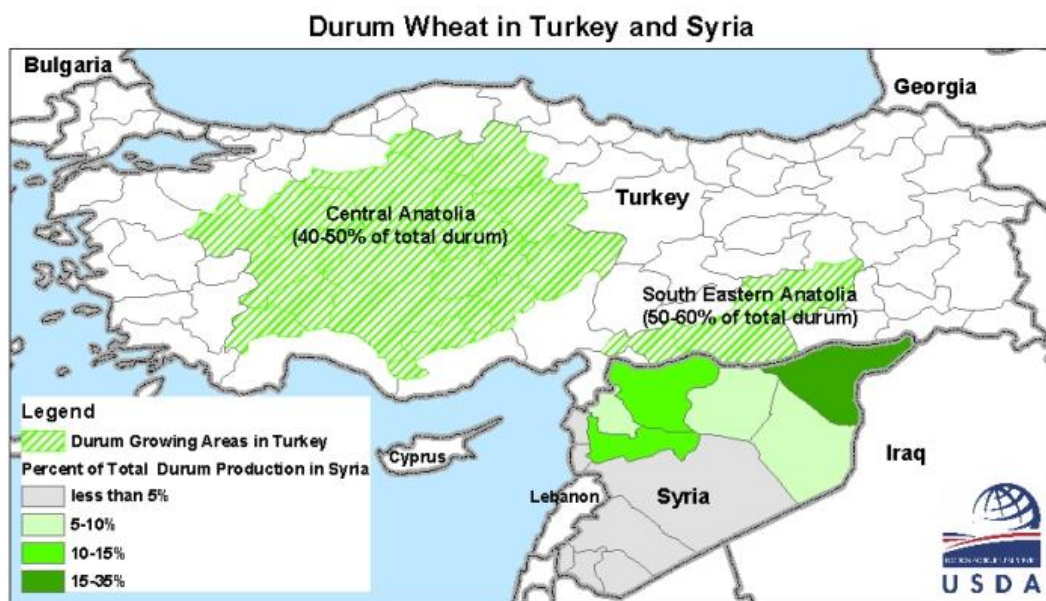


Figure 3: Durum Wheat Growing Areas

http://www.fas.usda.gov/pecad2/highlights/2003/11/durum%202003/Turkey_and_Syria.htm, Retrieved on 15/06/2011.

Durum wheat production in the Southeast Anatolia Region for 2010-2011 is estimated to be 1.2 million tons and in western Central Anatolia is estimated to be 1.1 million tons. Total durum production for Turkey is estimated to be 2.7 million tons for 2011 (<http://www.pecad.fas.usda.gov/highlights/2010/11/global%20durum/>).

1.1.4. Wheat Rust Diseases

The rust diseases are fungal diseases of wheat and have been the major biotic cause of yield losses (Saari & Prescott, 1985). They are the diseases that have attracted the most attention.

Fungal diseases are among the most catastrophic plant diseases. Since the parasitic fungi sporulate prolifically, they provide abundant number of inoculum to infect further. Also the production time for new spores after infection is very short, so they could infect new hosts in a short period of time. Besides, the spores can be spread in surface water or in water droplets by rain as well as they may be carried long distances by wind.

Rust fungi are obligate parasites, that is, they only survive on living plants. There are numerous races known to occur worldwide. There are three rust fungi of wheat and they belong to basidiomycete fungi of the genus *Puccinia* (McIntosh *et al.*, 1995). First one is stem or black rust which is caused by *P. graminis* f. sp. *tritici*. The second one is leaf or brown rust by *P. triticina* and the last one is yellow or stripe rust which is caused by *P. striiformis* f. sp. *tritici*. Each rust pathogen and its disease have their own global distribution and this distribution depends on environmental conditions in that specific area. The wheat rust fungi spread in the form of clonally produced dikaryotic urediniospores and they can be spread by wind even for long distances from their initial infection sites.

There are different races of rust fungi that can overcome different resistance genes of wheat to the particular disease. Also, new races may arise through sexual recombination (not known for *P. striiformis*), mutation, or somatic hybridization (Singh *et al.*, 2002).

1.1.4.1. Stem Rust

Stem rust, also known as black rust, is caused by the pathogen *Puccinia graminis* f. sp. *tritici* Eriks. &Henn. It is a destructing disease of durum (*Triticum turgidum* L.ssp. *durum*) and common wheat (*T. aestivum* L.) worldwide.

The stem rust fungus causes abundant production of shiny black teliospores that form in the uredinium at the end of the season. A healthy crop before harvest can be destroyed by development of stem rust if the fungi arrive from an infected wheat crop in a distant region.

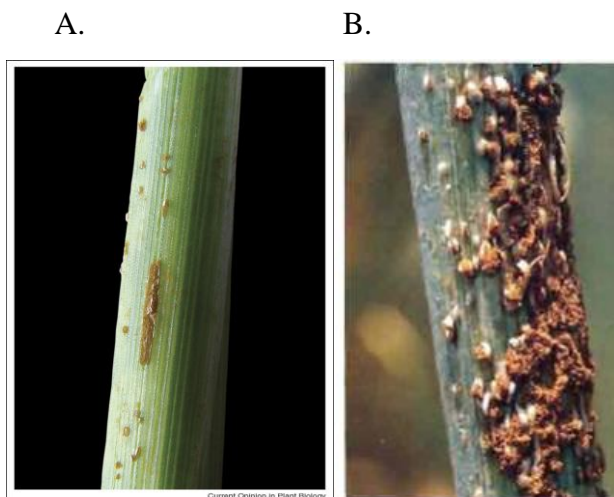


Figure 4. Examples of stem rust infection A: Wheat stem rust pustules of a Ug99 isolate that has mutated to overcome the Sr24 (resistance) gene taken from a field sample in Kenya. B: Uredinia of stem rust fungus *P. graminis* f. sp. *tritici* developed on a sensitive strain (after Ayliffe *et al.*, 2008).

1.1.4.1.1. Life cycle of Stem Rust & Infection Process

Puccinia graminis is heteroecious. This means the rust fungi that require two unrelated host plants, in this case wheat and barberry, to complete its life cycle. The fungus produces teliospores on the wheat plant which then produce a secondary spore, the basidiospore. This spore infects the barberry (*Berberis* spp.), which is a different host. Then a further spore stage, the aeciospore, is produced on the barberry which can reinfect the wheat. This infection causes the uredospore stage, which produces the actual symptoms on wheat.

Between the harvest of wheat crop in one season and grow of the next crop in other season, *P. graminis* can survive as dormant teliospores and these teliospores may give rise to new infections only on barberry. Without barberry as an alternative host, the teliospores are the dead end of fungus life cycle. When barberry grows near the wheat fields, they act as the alternative host for the spread of stem rust to the wheat again.

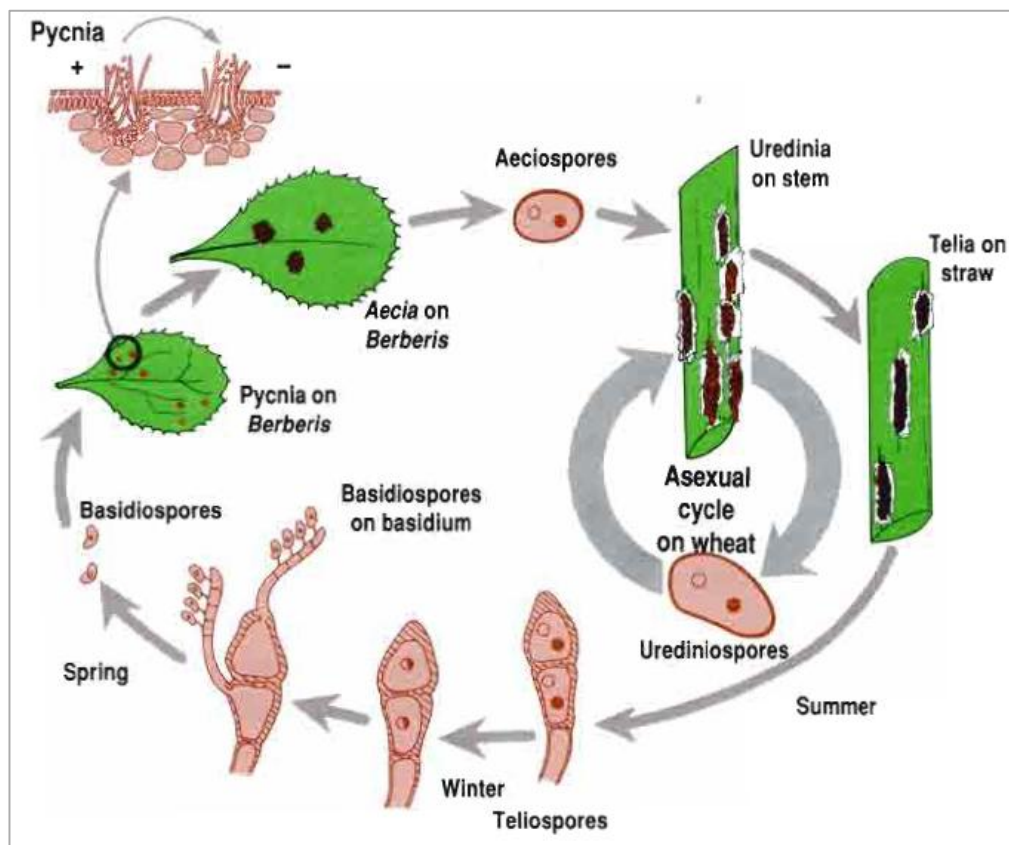


Figure 5. Life cycle of stem rust *Puccinia graminis* ssp. *tritici* (after Roelfs *et al.*, 1992)

Wheat shows the disease symptoms after ~10-15 days of infection and firstly oval pustules of brick-red urediniospores break through the epidermis. Although both wheat and barberry are required to complete the full life cycle, auto- can occurs on wheat infection and spores infect the same plant on which they are produced. By this property, the rapid development of disease occurs.

1.1.4.1.2. Stem Rust Epidemics in Turkey & in the World

Stem rust, caused by *Puccinia graminis* f. sp. *tritici*, has been an important fungal disease which cause yield losses on wheat. Any increase in severity of rust infection may cause a parallel increase in yield loss.

There have been serious epidemics happened. For example, in 1935 most of the wheat crops in North Dakota and Minnesota were lost due to stem rust disease (Leonard, 2001). Epidemics were developed in Australia in the 1940s and in the United States in the early 1950s (Luig & Watson, 1972; Saari & Prescott, 1985; Roelfs, 1986). The most severe epidemics in Europe occurred in 1932 and 1951 (Zadoks, 1963). Another stem rust epidemic had been observed in Iran during 1976. More recently, stem rust was observed in the Dozen and Gorgan regions adjacent to the Caspian Sea. Also, localized epidemics have been continuing to occur. There are numerous hotspots all over the world (Saari & Prescott, 1985).

Therefore, Saudi Arabia, Iraq, Iran and Afghanistan are all considered vulnerable to stem rust due to favorable environments and widespread cultivation of cultivars susceptible to race Ug99. Although there are not any devastating epidemics reported in Turkey, our country is considered to be in the region of Western Asia together with the countries mentioned above (CIMMYT, 2009).

Eradication of the alternate host (*Berberis vulgaris*) and use of stem rust resistant cultivars have contributed to the control of stem rust. However, in 1999, a new pathotype of stem rust was detected in Uganda and it was called race Ug99 (or TTKS) (Pretorius *et al.*, 2000). If the conditions are favorable for the pathogen, this race can spread to other wheat producing regions of world.

1.1.4.1.3. Genetic Resistance to Stem Rust

Resistance to wheat stem rust is dependent on single ‘gene-for-gene’ type resistance and there are 46 stem rust (Sr) resistance genes found to be in this type of resistance. It is known that gene-for-gene type resistance is based on a single resistance gene (R) product in the host which corresponds to an effector molecule produced by the pathogen. Most of the genes for resistance to rust are described in McIntosh *et al.*, (1995b).

Among the 46 stem rust resistance genes, only 20 were found originally in hexaploid bread wheat (*Triticum aestivum*). Nine of these genes were transferred to bread wheat from tetraploid *T. turgidum* (either wild or cultivated durum wheat) (McIntosh *et al.*, 1995).

Another class of wheat stem rust resistance genes are called adult plant resistance genes (APR) or slow rusting resistance genes. Normally, R genes act as single dominant genes to demonstrate resistance, thus, they are effective only to pathogen containing effector genes. However, APR genes act as quantitative traits. In other words, APR genes confer levels of disease resistance that when they come together they can even show immunity (Singh *et al.*, 2005). As understood from the name, APR genes usually provide resistance in mature plants, not in seedlings.

Rust severity is determined based on the infection types (ITs) after inoculation by using a 0 to 4 scale (Stakman *et al.*, 1962; Leonard & Szabo, 2005). The infection types are illustrated in Figure 6. ITs are; 0 (immune), 0;(fleck), 1 (small uredinia with necrosis), 2 (small uredinia with chlorosis), 3 (small uredinia without chlorosis or necrosis) and 4 (large uredinia without chlorosis or necrosis). The infection forms 0 to 2 are rated as resistant and 3 to 4 as susceptible.

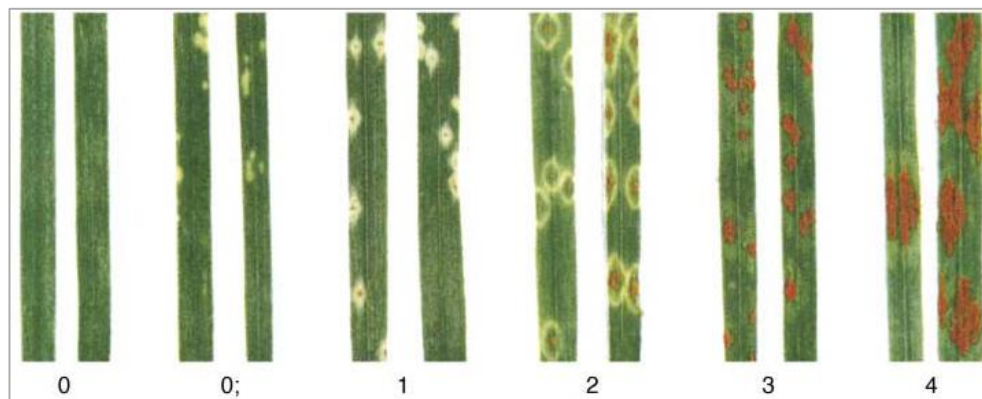


Figure 6. Infection types (ITs) of *Puccinia graminis* f. sp. *tritici* at a 0-4 scale (adapted from Stakman *et al.*, 1962)

1.1.4.2. Yellow rust (Stripe Rust)

Yellow rust or stripe rust is caused by the fungus *P. striiformis* f. sp. *tritici* which is an obligate biotrophic fungus like stem rust. It produces yellow colored pustules on the leaves of the plant.

Yellow rust infections are favored in cooler and humid regions. Thus, it is an important fact for temperate and maritime regions and higher elevations (Johnson, 1992).

It causes one of the most important wheat diseases together with stem rust in world, especially Asia, including Turkey over the last 25 years. Especially, when the environmental conditions are optimum, it can cause high yield losses (Roelfs, 1992).

Symptoms of the disease start to be seen in earlier spring. Yellow or orange-coloured pustules of the disease are formed mostly on leaves but they can be observed in other parts of the plant as well. The pustules may give rise to chlorosis and then necrosis

on leaves. Chlorosis occurs in a narrow yellow stripe which is parallel to the leaf veins. So the alternate name for this disease is stripe rust.

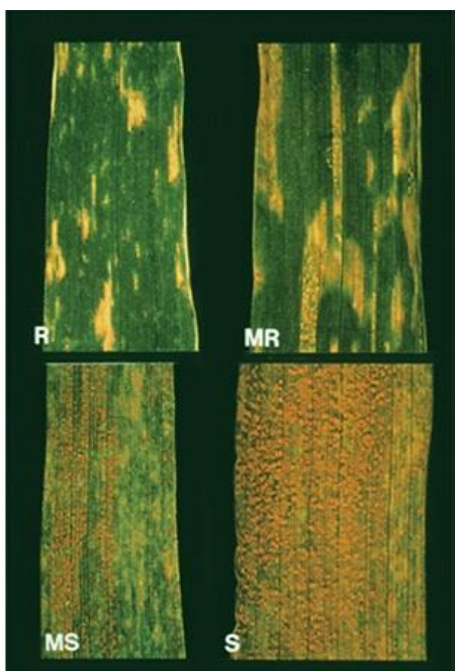


Figure 7. Relative resistances of wheat to yellow rust: R = resistant, MR = moderately resistant, MS = moderately susceptible and S = susceptible. Source: Rust Scoring Guide, Research Institute for Plant Protection, Wageningen, Netherlands. (after Marcalis & Goldberg, 2011)

1.1.4.2.1. Life cycle of Yellow rust & Infection Process

In the spring, when there is cool moist weather, the fungus *P. striiformis* f. sp. *tritici* starts to grow and produces active spores. The optimal conditions for spore germination and the spore production are 9-13 °C and a relative humidity of 100%.

Under normal circumstances, the cycle of infection till production of spores can last in 7 days. Therefore, the cycle can be repeated more than once in a growing season. During late summer, the dark teliospores could be produced. These teliospores can germinate to produce the basidiospore. Urediniospores are the only known source for inoculation for wheat. Alternate host for *P.striiformis* does not exist. For this reason, teliospores and basidiospores are not functional in life cycle of *P.striiformis*. Although the teliospores seem to have no function in the disease cycle, they can contribute to the development of new races via sexual recombination

(http://www.hgca.com/minisite_manager.output/3625/3625/Cereal%20Disease%20Encyclopedia/Diseases/Yellow%20%28Stripe%29%20Rust.msp?minisiteId=26),

Retrieved on 20/04/2011.

The disease essentially occurs on the leaves. Once the spores are released from a leaf, they can live for only a few days. They can infect only if conditions are suitable for germination. If temperature is low or high, time required for infection increases. Infection rarely occurs below 2°C, and ceases above 23°C. Glumes and base of the awns can also be affected (Muray *et al.*, 2005).

The spores are produced in huge numbers in pustules on the upper surface of leaves. Wind spreads the spores of yellow rust from pustules that develop on infected leaves. If the spores contact with another wheat leaf, they can germinate and infect that leaf.

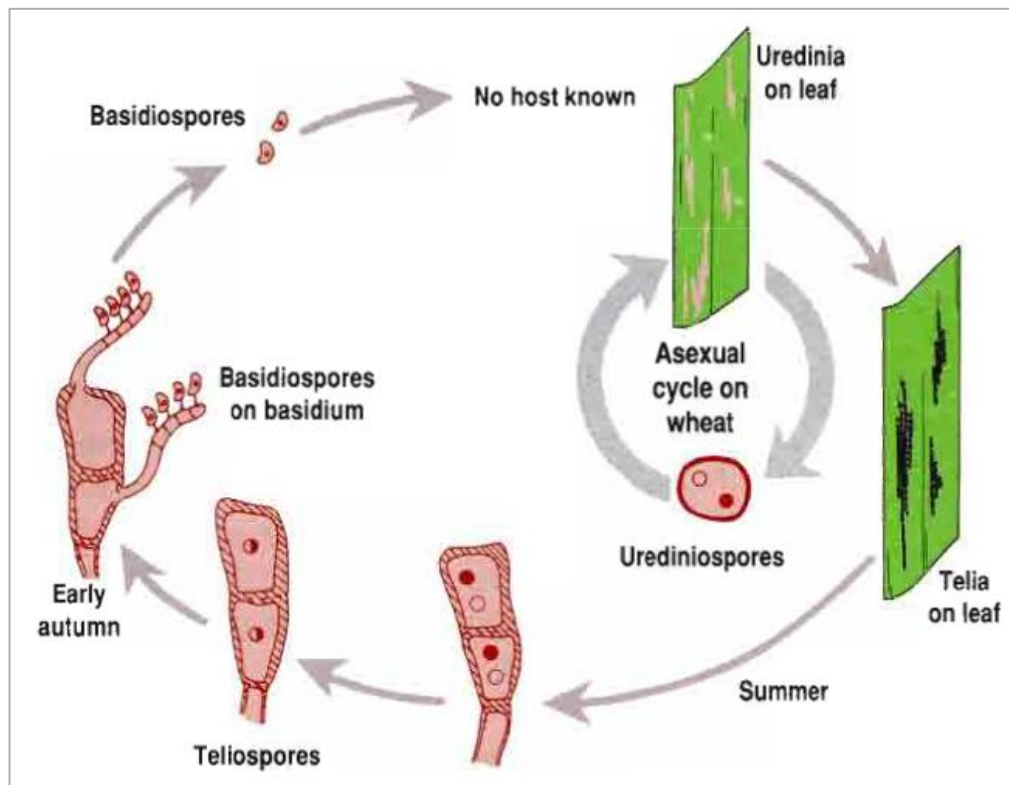


Figure 8. Life cycle of stem rust *Puccinia striiformis* f. sp. *Tritici* (after Roelfs *et al.*, 1992)

1.1.4.2.2. Yellow rust Epidemics

During the 1980s and 1990s, the world wheat experienced a series of major epidemics of wheat yellow (stripe) rust because there was a breakdown of the yellow rust resistance gene Yr9. This gene is present in several cultivars grown in South, West and Central Asia. Thus, the loss of this resistance caused huge amount of crop losses.

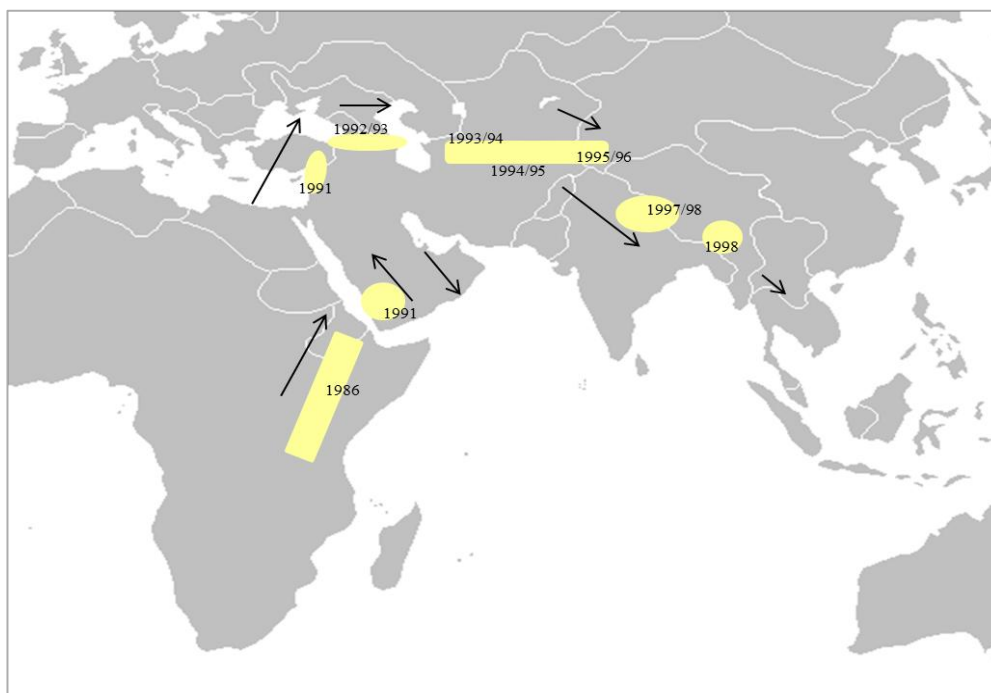


Figure 9. The gradual spread of the Yr9-virulent wheat yellow rust from eastern Africa to the South Asia (CIMMYT, 2005).

As seen in Figure 9, the entire wheat area in Asia (except China) is an epidemiologic zone that is connected to Eastern Africa. Therefore, if a new race of yellow rust fungus overcomes the present resistance, it could spread all over the epidemiologic region (CIMMYT, 2005).

Yellow rust was observed in northern Europe, the Middle East, East Africa, China and India, the west coast of the USA, the Andean region of South America, Australia and New Zealand (Saari & Prescott, 1985).

Among the fungal diseases causing yield losses, yellow rust caused by *P. striiformis* f. sp. *tritici*, is the most widely distributed one. In Turkey, yellow rust is mostly observed in the cooler plateaus of central and eastern Anatolia, Thrace, and

mountainous areas (Iren, 1981). There were yellow rust epidemics that had been reported in Turkey and other countries (Kınacı & Kınacı, 1991; Mamluk, 1992; Canhos *et al.*, 1997). For instance, yellow rust virulence for 8156 cultivars has migrated from Turkey to the Middle East; Pakistan and India (Figure 10).

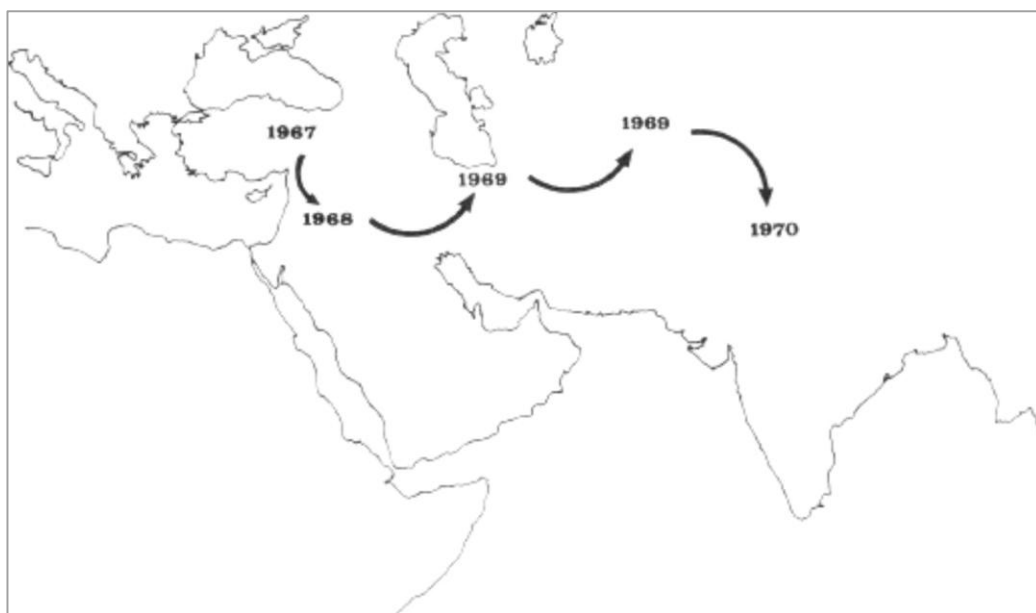


Figure 10. Years of the first recorded appearance of the *Puccinia striiformis* virulence for 8156 cultivars and its possible migration path (after Saari & Prescott, 1985).

1.1.4.2.3. Genetic Resistance to Yellow rust

Genotypes of wheat have been classified as resistant, moderately resistant, moderately resistant–moderately susceptible, moderately susceptible, moderately susceptible–susceptible and susceptible to the yellow rust disease (Pasquini *et al.*, 1998).

Resistance to yellow rust can be divided into two as all-stage resistance (seedling resistance) and as adult-plant resistance. All stage resistance (seedling resistance) is observed at the seedling stage, but it is also shown in other stages of plant growth. On the other hand, adult plant resistance is expressed at later stages of plant growth. All stage resistance is race specific (Chen & Line, 1992a, 1992b, 1993; Chen *et al.*, 1995b, 1998a). It is effective only when there is a resistance gene in the cultivar genome against *P. striiformis* f. sp. *tritici* carrying the corresponding avirulence gene. This type of resistance is compatible with the description of the gene-for-gene hypothesis first proposed by Flor (1942). So cultivars with all-stage resistance can be sensitive to new races of the fungus that can emerge (Line & Qayoum, 1992; Line & Chen, 1995, 1996).

There is another type of resistance to the yellow rust disease. It is the high-temperature adult-plant resistance (HTAP). This resistance is durable and it is not race specific (Qayoum & Line, 1985; Milus & Line, 1986a, 1986b; Line & Chen, 1995; Chen & Line, 1995a, 1995b; Chen *et al.*, 1998a). Cultivars having only HTAP resistance are susceptible to pathogen at the seedling stage. However, as the plant grows and temperature increases during the growing season, the plant becomes resistant. HTAP resistance lowers the infection type, prevents new infections and stops spread of inoculum. For cultivars with the highest degree of HTAP resistance, sporulation is completely inhibited (Chen & Line, 1995a, 1995b).

There are seventy genes (*Yr* followed by a number or *Yr* followed by letters) reported for yellow rust disease. Most of these genes are unique and most of the known genes show all-stage resistance. There are also many genes that have not been named yet (Chen *et al.*, 1998a; Chen, 2002).

1.1.4.3. Breeding Wheat for Rust Disease Resistance

Achieving high resistance to fungal diseases is an ongoing challenge for wheat breeding. To increase the resistance of wheat to diseases various aspects are considered. Attempts for understanding pathogen biology, characterization of avirulence and resistance genes and research for new resistance sources contribute to the development of wheat with increased resistance to various diseases.

Although rust diseases are mostly controlled by resistant cultivars, virulent pathotypes are continuing to be threats. Almost most of the research is directed to identify and utilize sources of resistance that are considered to be durable (Simmonds & Rajaram, 1988). Durable resistance is the resistance that remains effective over many years and can only be recognized retrospectively (Johnson, 1984).

When environmental conditions are favorable and wheat varieties susceptible, fungal diseases may cause severe epidemics resulting in yield losses of over 60 percent. Wheat rusts can be controlled worldwide by planting resistant varieties of wheat. Fungicides may be effective, but for wheat rusts, they are not economical because pathogens may evolve to develop resistance to fungicides, making them ineffective. Murray & Brennan (2009) estimated the cost of fungicides for foliar cereal disease control in Australia in 2008 to be approximately US \$8/ha except the application costs.

During the 1980s and 1990s, the world experienced a series of major epidemics of wheat yellow (stripe) rust due to a breakdown of the yellow rust resistance gene Yr9, present in several cultivars that were grown in South, West and Central Asia. This caused huge amount of crop losses. Recently, *Puccinia graminis* f. sp. *tritici* race Ug99 and its derivatives showed risk of stem rust disease (Pretorius *et al.*, 2000; Web page of International Maize and Wheat Improvement Center (available online at http://www.globalrust.org/db/attachments/resources/737/10/BGRI_2009_proceeding_s_cimmyt_isbn.pdf, last access date: April 2011).

Furthermore, rust fungus is easily transported short distances by wind gusts, which puts most of the countries in Near East (i.e. Egypt, Iraq, Jordan, Lebanon, the Syrian Arab Republic and Turkey) at similar risk.

Moreover, Turkey is accepted under the category of countries at high risk according to FAO's wheat rust disease global program (FAO, 2008). Therefore, an urgent attempt should be made to enhance the use of resistant varieties which is the only effective option to prevent rust epidemics because chemical control is not affordable and effective (Joshi *et al.*, 2008; Singh *et al.*, 2008).

Since rust spores can travel long distances, new races may easily migrate to other countries. For example, Yr9-virulent race of *P. striiformis* travelled from the East African highlands to the Indian subcontinent between 1985 and 1997 and then reached Nepal (Duveiller *et al.*, 2007).. This is an example of spread of the yellow rust disease. Also, earlier than this, virulent strains for the *Yr2* gene, travelled from Turkey to Pakistan (Singh *et al.*, 2002, 2005).

Resistance breeding is the most effective way of preventing rust diseases. It is also the most economical and ecologically friendly approach to avoid yield losses. It is important to identify and characterize resistance sources and it is urgent to employ resistance sources. Genetic resistance is the main method to control the rust parasites. However, disease control requires use of durable and race nonspecific resistance together with high yielding genotypes.

Although the genetics of resistance to plant disease was first explained in 1905 (Faris *et al.*, 2008), selection for disease resistance is an ongoing challenge for breeders since the beginning of agriculture. Resistance genes can be introduced by hybridization. When the genetic resistance is obtained, it is easy and cheap to control. More precisely, it is important to have durable resistance in cultivar, a concept proposed by Johnson (1984). Durable resistance, i.e., the resistance that remains effective over many years, can only be recognized retrospectively.

Moreover, resistance that is proved to be durable by experience can be used in breeding programs. Breeding plants with resistance against a specific disease firstly requires the identification of resistant plants. These resistant ones are crossed with the ones having agronomic importance but disease susceptibility. Then, the new generation is backcrossed to the susceptible parent and resistant phenotypes are selected. At the end of the procedure, new cultivar is obtained which is similar to the susceptible parent, but has the required resistance. This process takes long time and in this period the pathogen could evolve so that, it is not recognized by the hybrid cultivar (Strange & Scott, 2005).

1.2. Spectroscopy

1.2.1. Electromagnetic Radiation and Optical Spectroscopy

Light is in the form of electromagnetic radiation. Electromagnetic radiation is considered to behave as two wave motions, which are perpendicular to each other. One of these waves is magnetic (M) and the other one is electric (E). These perpendicular components oscillate sinusoidally as they propagate through space as shown in Figure 11 (Stuart, 1997).

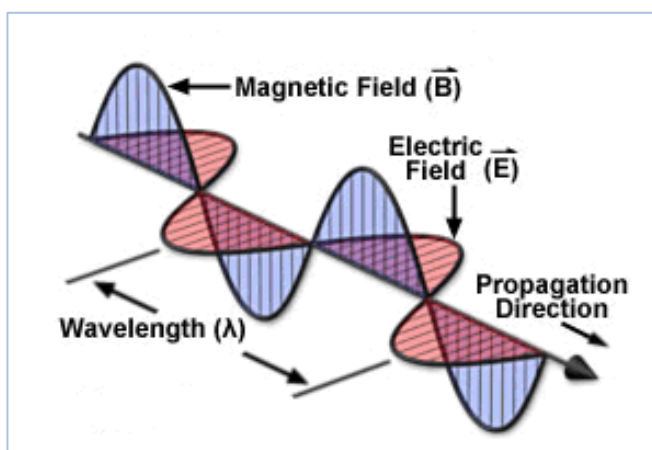


Figure 11. An electromagnetic wave

(<http://micro.magnet.fsu.edu/primer/java/electromagnetic/index.html>), Retrieved on 01/09/2011.

When the light interacts with matter, it can be scattered (i.e., its direction of propagation changes), absorbed (i.e., its energy is transferred to molecule) or emitted (i.e. energy is released by the molecule).

If the electromagnetic energy of light is absorbed by a molecule, it becomes excited. It can be said that the molecule is in an excited state. An excited molecule has any one of a set of discrete amounts (quanta) of energy. This energy is described by the laws of quantum mechanics. The energy amounts are called energy levels of the molecule. The major energy levels are determined by the possible spatial distributions of electrons, which are called electronic energy levels. There are also vibrational energy levels which are superimposed on electronic energy levels and these are results of the various modes of vibration of the molecule such as stretching and bending of chemical bonds. All of these energy levels are described by an energy level diagram (Figure 12).

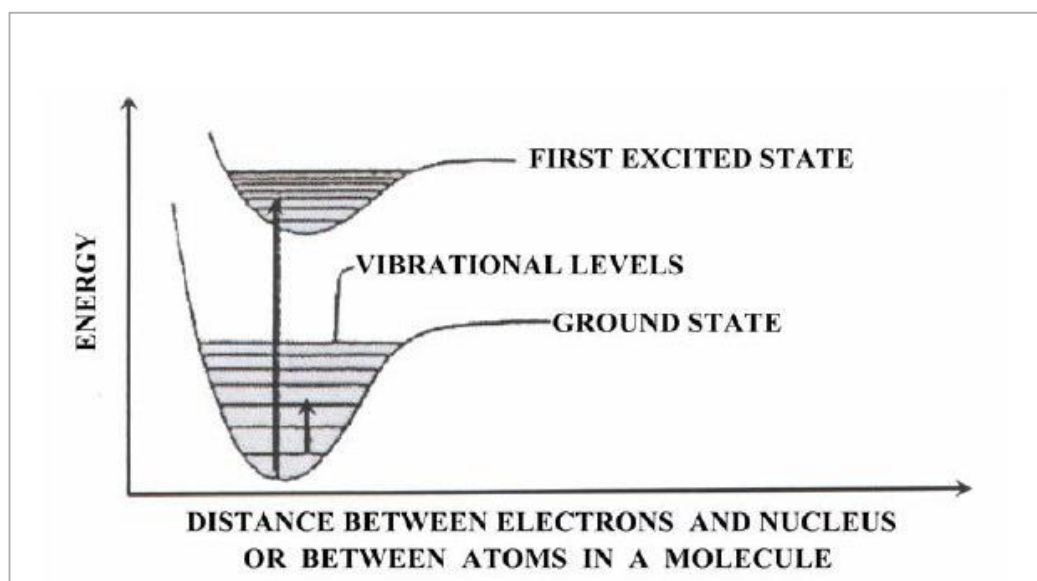


Figure 12. Typical energy-level diagrams showing the ground state and the first excited state. Vibrational levels are shown as thin horizontal lines. A possible electronic transition between the ground state and the fourth vibrational level of the first excited state is indicated by the long arrow. A vibrational transition within the ground state is indicated by the short arrow (Freifelder, 1982).

In the energy level diagram, the lowest electronic level is the ground state and all other electronic levels are excited states. The horizontal lines in energy level diagram represent the vibrational levels. A change between the energy levels is called a transition. The long arrow in the figure shows a possible electronic transition while the short arrow represents a vibrational transition within the ground state (Freifelder, 1982).

The transitions can occur only if there is a strong interaction between the incident radiation and the molecule itself. Absorption is most probable when the energy level separation matches with the energy of the incident radiation.

The energy of electromagnetic wave is;

$$\Delta E = h\nu \quad (1)$$

in which ΔE is the separation between the energy states of interest, ν is the frequency of the applied radiation and h is Planck's constant (6.6×10^{-34} joule second)

$$c = \lambda \nu \quad (2)$$

in which c is speed of light in vacuum (3.0×10^8 ms⁻¹) and λ is the wavelength of light.

The expression of radiation as a function of frequency in Hz gives us huge numbers which is harder to deal with. Therefore, we can define another unit wavenumber ($\bar{\nu}$) which is the inverse of wavelength in centimeters. It is the number of waves per centimeter.

$$\bar{\nu} = \text{wavenumber} = (1/\lambda) \text{ [has a unit of cm}^{-1}\text{]} \quad (3)$$

$$E = h \nu = h c \bar{\nu} \quad (4)$$

From the above equations, it is obvious that both frequency and wavenumber are directly proportional to the energy.

Spectroscopy is defined as the study of the interaction of electromagnetic radiation with matter. Spectroscopic techniques involve irradiation of a sample with some form of electromagnetic radiation, measurement of the scattering, absorption, or emission in terms of some measured parameters, and the interpretation of these measured parameters to give useful information. Figure 13 illustrates the important regions of the electromagnetic spectrum.

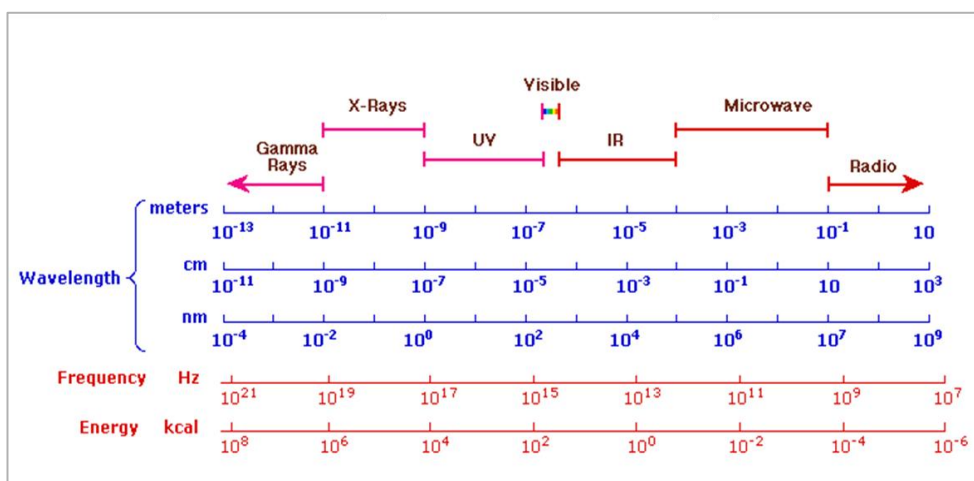


Figure 13. The Electromagnetic spectrum

For most purposes, it is convenient to think that a molecule as if it possesses several distinct reservoirs of energy. The total energy is given by:

$$E_{\text{total}} = E_{\text{translation}} + E_{\text{rotation}} + E_{\text{vibration}} + E_{\text{electronic}} + E_{\text{electron spin orientation}} + E_{\text{nuclear spin orientation}}$$

Each E in the equation represents the appropriate energy as indicated by its subscript. The contributions of $E_{\text{translation}}$, $E_{\text{electron spin orientation}}$ and $E_{\text{nuclear spin orientation}}$ are negligible because the separations between respective energy levels are very small.

1.2.2. Basis of Infrared Spectroscopy

Infrared (IR) spectroscopy is the spectroscopy that deals with the infrared region of the electromagnetic spectrum. Generally, the main experimental parameter is wavenumber ($\bar{\nu}$). The infrared region of the electromagnetic spectrum is usually divided into three sub-regions; the near, middle and far infrared (Smith, 1999);

<u>Region</u>	<u>Wavenumber Range (cm⁻¹)</u>
Near	14000-4000
Middle	4000-400
Far	400-4

This spectroscopic technique gives information on molecular vibrations. The transitions between vibrational levels of the ground state of a molecule result from the absorption of electromagnetic radiation energy of light in the infrared (IR) region, which is shown in Figure 12.

For the absorption of infrared to occur, the vibration should cause a change in the electric dipole moment which means that there must be a displacement of charge across bond. This happens only when two oppositely charged molecules get closer or move further apart as the bond bends or stretches. Thus, infrared spectrum is generated by the characteristic motions of the functional groups such as methyl, carbonyl and amide.

The characteristic motions include bond stretching and bond bending. A stretch produces a change in bond length because it is a movement along the line between the atoms in which the interatomic distance is either increasing or decreasing. The bending results in a change in bond angle. Both stretching and bending vibrations can have variations. A stretch can be symmetric or asymmetric. Bending can occur in the plane of the molecule or out of plane and it can be scissoring, like blades of a scissor or rocking, in which two atoms move in the same directions (Volland, 1999). Figure 14 demonstrates the molecular vibrations of a triatomic molecule.

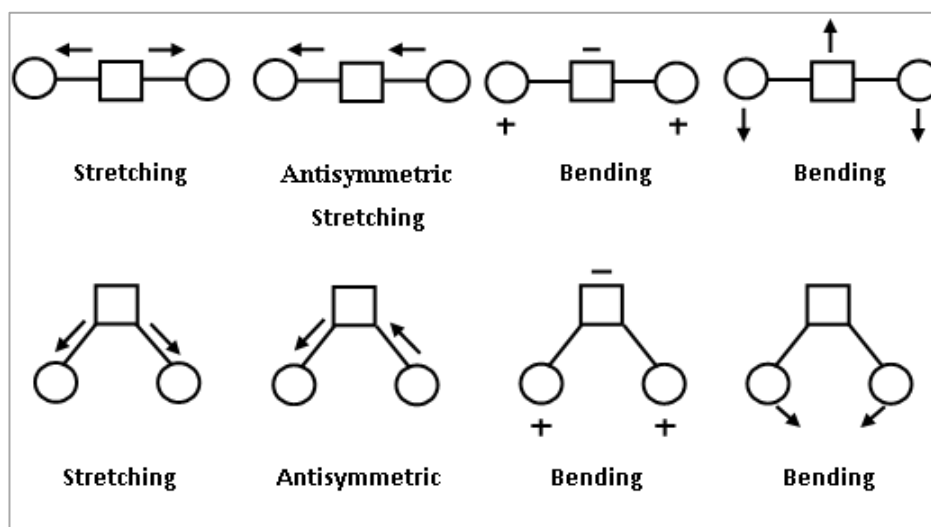


Figure 14. The schematic representation of some molecular vibrations in linear triatomic molecules and non-linear triatomic molecules. (+) and (-) symbols represent atomic displacement out of page plane (Arrondo *et al.*, 1993).

In infrared spectral analysis the modes of vibration of each group are very sensitive to the changes in chemical structure, conformation and environment. In addition, since each material has a unique combination of atoms, it is impossible that two compounds produce the exact same infrared spectrum. Therefore, an infrared spectrum can be used in identification of every different kind of material.

1.2.2.1. Fourier Transform Infrared Spectroscopy (FTIR)

Fourier Transform Infrared (FTIR) Spectroscopy is a widely used method for analyzing molecular structure and structural interactions in biological systems. It measures absorption of vibrations of molecules. The vibrations result from energy transitions of vibrating dipoles. It is a powerful technique to investigate the detailed structural changes in molecules because very small changes in bond lengths and angles can be detected. With the progress in FTIR spectrometer, applications of IR

spectroscopy have been expanded to study biological molecules. The FTIR technique has the advantage of rapid recording of high resolution, low-noise spectra even in aqueous medium. The data acquisition process is automated (Toyran *et al.*, 2006).

An FTIR spectrometer consists of a fixed mirror, a moving mirror and a beam splitter, as shown in Figure 15.

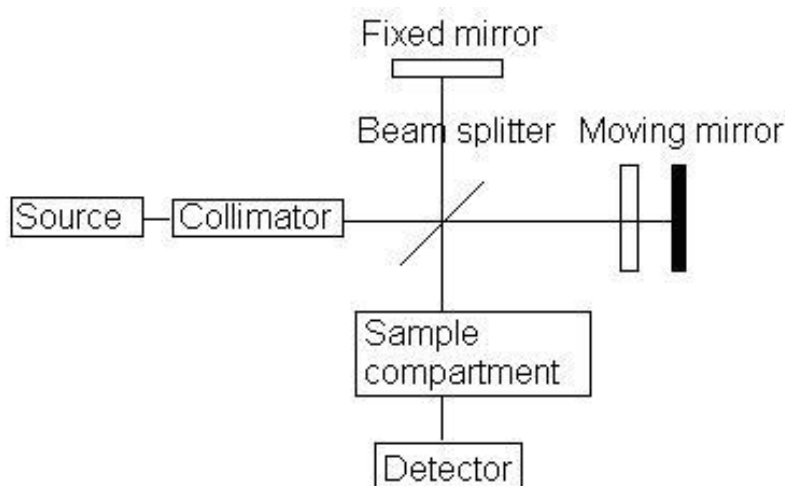


Figure 15. Basic components of FTIR spectroscopy
(<http://optometry.college.edu.pe>), Retrieved on 5/05/2011.

The collimated IR beam from the source is partially transmitted to the moving mirror and partially reflected to the fixed mirror by the beam splitter. The two beams are recombined when they meet back at the beam splitter. The detector detects the transmitted beam from the fixed mirror and reflected beam from the moving mirror simultaneously. The signal which exits the interferometer is the result of the two beams interfering with each other. The resulting signal is called an interferogram.

In interferogram every data point forming the signal has information about every infrared frequency coming from the source. This means that as the interferogram is measured; all frequencies are being measured simultaneously. But the interferogram signal cannot be interpreted directly. It is converted to frequency information by using Fourier transformation. This transformation is done by the computer and spectral information is formed for analysis.

The FTIR spectrum is usually represented as plot of intensity versus wavenumber (in cm^{-1}). Wavenumber is the reciprocal of the wavelength. The intensity can be plotted as the percentage of light transmittance or absorbance at each wavenumber.

1.2.2.2. The Advantages of FTIR Spectroscopy

Fourier transform infrared (FTIR) spectroscopy is more sensitive, rapid, and more environmentally friendly compared to other chemical methods (Kamnev, 1998). It is also a non-invasive technique that gives not only qualitative and quantitative information about the chemical structure, but also information about molecular conformation and interaction between neighboring molecules. Thus, this technique detects macromolecular compounds such as proteins, lipids, carbohydrates, and nucleic acids, simultaneously (Kamnev, 1998; Bourdon, 2000; Yang, 2002; Cakmak, 2003; Zdrov, 2003; Toyran, 2004).

The other advantage of FTIR spectroscopy is that spectra of almost any biological material can be obtained in different environments. There is no light scattering or fluorescent effects and this technique is not as expensive as X-ray diffraction, NMR, ESR and CD spectroscopic equipment (Haris & Severcan, 1999).

Another advantage of FTIR spectroscopy lies in its ability to increase signal to noise ratio by signal averaging (Stuart, 1997). It is possible to improve signal-to-noise ratio (noise adds up as the square root of the number of scans, whereas signal adds linearly) by the use of computer. Also, the data processing is simple with the

computer software. Moreover, data storage, alterations on data and quantitative calculations are allowed in this technique (Rigas *et al.*, 1990; Manoharan *et al.*, 1993; Yono *et al.*, 1996; Ci *et al.*, 1999).

Sample preparation is very easy. Samples can be prepared in gaseous, liquid, or solid states (solutions, viscous liquids, suspensions, nonhomogeneous solids or powders) (Colthup *et al.*, 1975). The technique can be applied to the analysis of any kind of biological material and it is not limited to the physical state of the sample. The amount of sample required is relatively small and it is a non-destructive technique (Haris & Severcan, 1999; Melin *et al.*, 2000; Çakmak *et al.*, 2003). It provides a precise measurement method, which does not require any external calibration.

In FTIR spectroscopy, rapid data acquisition and qualitative interpretation is possible. Moreover, due to different technology of FTIR spectroscopy, it is possible to examine the functional groups that are not accessible with ultraviolet and visible light absorption spectrometers (Freifelder, 1982).

Attenuated total reflectance (ATR) Spectroscopy functions by sending a wave to the sample through an ATR crystal, which is usually Germanium, Silicon, Zinc selenide (ZnSe) or diamond. In this technique, sampling is simpler and non-destructive because the sample need not be mixed with another material.

1.2.2.3. Attenuated Total Reflectance (ATR) FTIR Spectroscopy

In FTIR spectroscopy, IR beam passes through the sample whereas in ATR spectroscopy the beam is totally reflected at the interface of the two surfaces. The beam then contains spectral information about the sample fixed onto the reflection element.

An attenuated total reflection FTIR spectroscopy measures the changes that occur in an internally reflected infrared beam when the beam comes into contact with a

sample. The infrared beam collides to an optically dense crystal with a high refractive index at a certain angle. Then, an evanescent wave is formed beyond the surface of the crystal which is in contact with the sample held on the crystal.

The sample must be in direct contact with the ATR crystal surface because the evanescent wave only extends beyond the crystal. In regions of the infrared spectrum where the sample absorbs the energy, the evanescent wave will be attenuated or altered. This attenuated energy from each evanescent wave is passed back to the infrared beam, which then exits the opposite end of the crystal. Then, the detector in the infrared spectrometer detects that beam. The system generates an infrared spectrum. In ATR-FTIR spectroscopy it is important to have a crystal with the appropriate refractive index (Merket *et al.*, 1998; Dubis *et al.*, 1999; Dubis *et al.*, 2001). The refractive index of the crystal must be greater than that of the sample. For fresh and especially water-bearing plant materials the recent technique called attenuated total reflectance (ATR) can be used for collecting spectrum of the leaf structure.

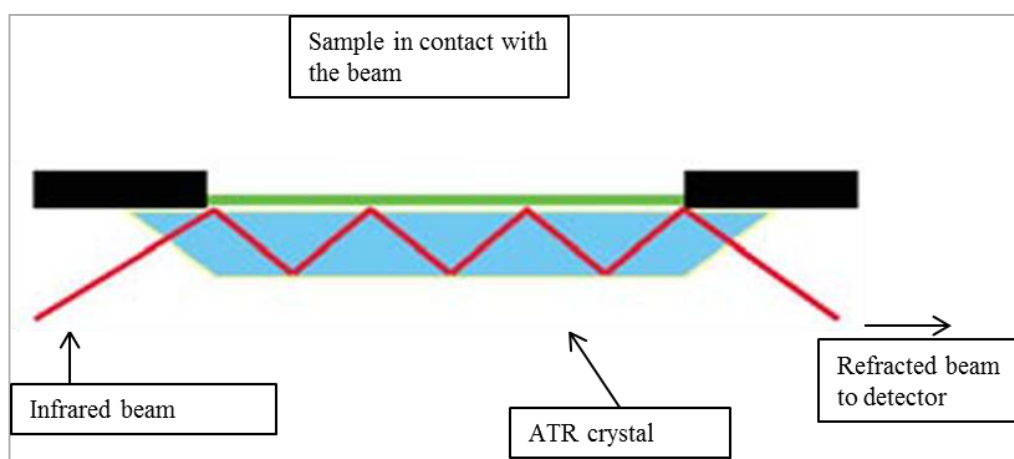


Figure 16. A multiple reflection ATR system

1.2.2.4. The Use of FTIR Spectroscopy in Plant Classification and Identification

FTIR spectroscopy is a highly preferred technique in classification and identification of plants. It has sensitive and non-invasive technology giving information about chemical structure, molecular conformation and interactions between biomolecules, rapidly.

In FTIR spectroscopy, the groups or the bonds of the molecules have characteristic bands in an infrared spectrum. These characteristic bands are assigned to particular groups in biomolecules. Therefore, the spectra obtained could be examined for several groups depending on the group frequency.

Since FTIR spectroscopy enables the investigation of the vibrations originating from biochemical components, such as lipids, proteins, nucleic acids, and carbohydrates, identification can be done by infrared spectroscopy via searching for specific plant components and chemical similarities in leaves, fruits or other parts of the plants.(Da Luz, 2006). For instance, by using FTIR spectroscopy tomato cultivars can be classified based on their sugar (glucose, fructose and sucrose) and organic acid (citric acid, malic acid, tartaric acid, fumaric acid and succinic acid) contents (Beullens *et al.*, 2006). Also, detailed chemical composition of marama bean, which have commercial importance, was analyzed by this technique (Holse *et al.*, 2011). As FTIR spectroscopy serves as a rapid alternative to chemical methods for authentication and quantification of coffee products, *Coffea Arabica* and *Coffea Canephora* variant *Robusta* were studied in order to compare their flavor qualities by this technique (Kemsley *et al.*, 1996).

In addition, phylogenetic discrimination of plant species was done based on their biophysical profiles by infrared spectroscopy. For example, leaf samples of Rosaceae family, Crassulaceae family, Apocynaceae family and Liliaceae family species and varieties were studied by FTIR spectroscopy to determine their phylogenetic relationships and they are classified depending on their FTIR spectra (Kim *et al.*,

2004). In the other study, *Ranunculus* (Ranunculaceae), *Acantholimon* (Plumbaginaceae) and *Astragalus* (Leguminosae) genera species of Turkey were studied and discriminated based on their compositional and structural differences in their biomolecules (Gorgulu *et al.*, 2007). Furthermore, cultivars of olives picked up in the Moroccan region of Beni Mellal were subjected to a characterization and classification study and they are separated into different classes based on their FTIR spectral characteristics (De Luca *et al.*, 2011). Moreover, the discrimination and classification of allergy relevant pollens were studied by Fourier transform infrared (FT-IR) microspectroscopy and different allergenic pollen taxa were classified based on the infrared spectra (Dell'Anna *et al.*, 2009). The pollen samples of order Pinales have also been studied to classify and by using both the transmission FTIR spectroscopy via KBr pellet and ATR-FTIR spectroscopy. In this study, it was shown that biochemical similarities of pollen grains that belong to same genus or family reflect similar features in corresponding spectra (Zimmermann, 2010).

There are also FTIR studies in which wheat species were studied. The presence of Deoxynivalenol (DON), which is a mycotoxin produced by fungi, was searched with Fourier transform near-infrared spectroscopy (FT-NIR) in durum and common wheat (De Girolamo *et al.*, 2009). The changes in protein content and amount were monitored during maturation of developing grains of wheat non-destructively by near infrared spectroscopy (NIR) (Gergely & Salgo, 2007). Since the technique is capable of determining the composition of biological material, it was successfully used in identification of cell wall materials of wheat (Saulnier *et al.*, 2005; Guillon *et al.*, 2006).

1.3. Objective & Justification of the study

The rust diseases are among the most catastrophic diseases of wheat which can cause great amount of yield loss. From past to present, breeding efforts have been directed to obtain durable resistance in cultivars that are also economically important.

In breeding studies, the cultivars that are determined to be resistant to a particular disease are used in crosses between the susceptible, but with agronomically important traits. Then, the new generation materials are backcrossed to the susceptible parent and the resistant ones are selected from the following generation. These resistant lines have both the required resistance to the disease under consideration and the characteristics that are important in agricultural productivity. However, these new resistant lines should be exposed to the rust disease pathogen in field and the resistance should be confirmed. These breeding strategies take long time, even years, which makes it difficult to obtain the desired cultivars because by the time the pathogen could evolve and the hybrid obtained cannot recognize this new pathotype. Because of these, the identification of cultivars as resistant or sensitive is urgent. Hence, in this study we used FTIR spectroscopy, which gives reliable and rapid molecular information.

This study aims to investigate the molecular differences between resistant and sensitive RILs of stem rust and yellow rust diseases by using ATR-FTIR spectroscopy. FTIR spectroscopy is a sensitive and rapid technique for molecular structure and conformation and interaction studies. Besides, it is a non-invasive method for classification and discrimination studies. By using FTIR technology, one can obtain rapid and reliable data on the molecular structure and conformation of the biological molecule under consideration.

Since the positions and areas of many of the infrared absorption bands can be correlated with the presence of specific groups of atoms in the system studied (Steele, 1971), it is possible to assign specific wavelength molecular absorption

bands to specific vibrational modes of particular functional groups. In this study, the same approach was applied to the spectra obtained. Thus, the goal in the study is to search for any spectral difference in molecular absorptions and to determine whether these can be used as molecular markers for the stem rust and yellow rust disease resistance in durum wheat or not.

CHAPTER 2

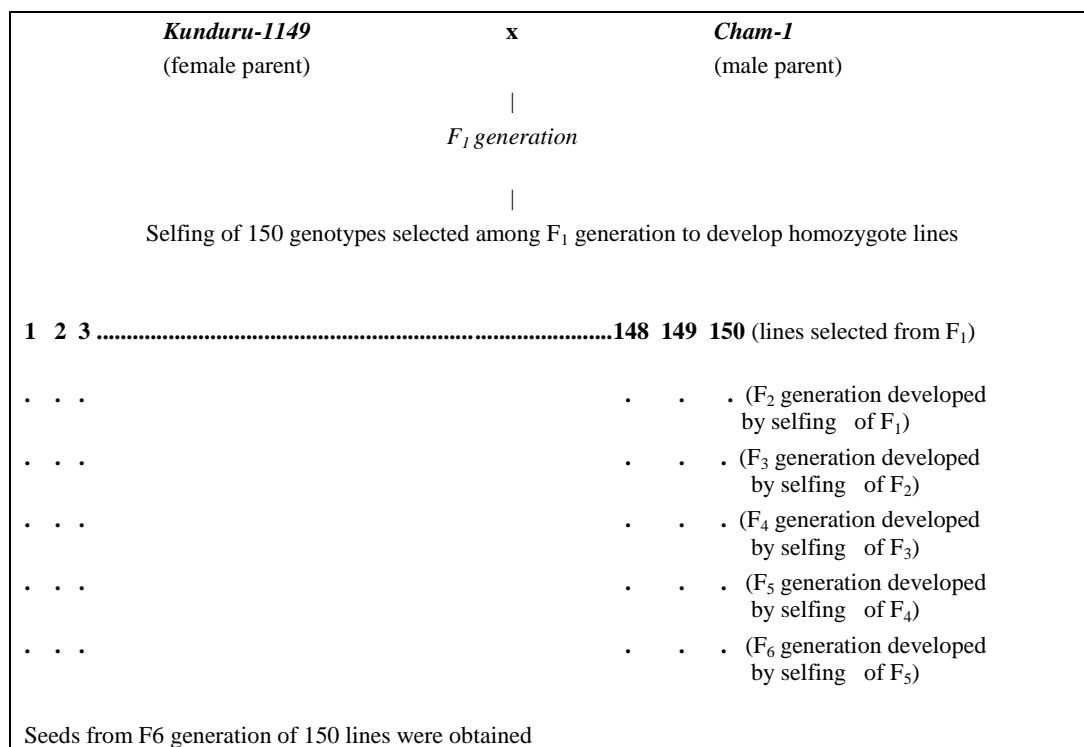
MATERIALS AND METHODS

2.1. Plant materials, assessments of yellow and stem rusts

F6 recombinant inbred lines (RIL) which were developed in International Center for Agricultural Research in the Dry Areas (ICARDA) in Aleppo, Syria were used in this study. The population was developed from a cross of Kunduru-1149 and Cham-1 (Table 2) (Göçmen *et al.*, 2003).

The female and male parents of the population developed are Kunduru-1149 and Cham-1, respectively. Kunduru-1149 has cold tolerance and high quality of yield but the yield of this parent is very low and also it is susceptible to the disease. In contrast, male parent Cham-1 has cold susceptibility and the quality of the yield is low, while it gives high yield and it is resistant to the disease (Göçmen *et al.*, 2003).

Table 2. Development of 150 lines of F₆ progeny of Kunderu-1149_Cham-1 cross (Göçmen *et al.*, 2003)



The performance of 150 RILs and the parents were evaluated in previous studies (Göçmen *et al.*, 2003; unpublished thesis), to designate their resistance states to stem and yellow rust diseases according to the modified Cobb Scale. In this scale, the reaction intensity was evaluated from 1 to 100 and the lines were categorized as R (resistant; necrotic areas with or without small pustules), MR (moderately resistant; small pustules surrounded by necrotic areas, MS (moderately susceptible; medium-sized pustules, no necrosis, but some chlorosis possible, S (susceptible; large pustules, no necrosis or chlorosis). Then, this nomenclature is converted to coefficient of infection values by using; R=0.2, MR=0.4, MR-MS=0.6, MS-MR=0.6, MS=0.8, MS-S=0.9, S-MS=0.9 and S=1.0 for statistical analysis (Göçmen *et al.*, 2003).

2.2. Sample Selection & Preparation for ATR-FTIR spectroscopy

40 durum wheat RILs (20 stem rust resistant and 20 stem rust sensitive) were used for spectroscopic analysis of stem rust disease and 40 durum wheat RILs (20 yellow rust resistant and 20 yellow rust sensitive) were used for spectroscopic analysis of yellow rust disease. These 40 RILs were grouped as resistant and sensitive cultivars based on the results of previous studies (Göçmen *et al.*, 2003; unpublished thesis on stem rust). For each resistant or sensitive RIL, 3 randomly chosen seeds were grounded by freeze grinder with the frequency of 17 for 2 minutes under liquid nitrogen.

2.3. ATR-FTIR spectroscopy

In ATR-FTIR Spectroscopy measurements 0.1mg of each sample per each RIL is used and 150 gauge pressure was applied. Infrared spectra were obtained using a Perkin-Elmer Spectrum One FTIR spectrometer (Perkin-Elmer Inc., Norwalk, CT, USA) equipped with a MIRTGS (Middle infrared TriGlycine Sulfate) detector. Water and carbon dioxide molecules in the air affect the IR spectrum. To overcome these problems the spectrum of air was recorded as background and subtracted automatically by using appropriate software (Spectrum One software-Perkin-Elmer Inc., Norwalk, CT, USA).

The spectra of samples were recorded in 4000-650 cm^{-1} region at room temperature. Each interferogram was collected with 100 scans at 4 cm^{-1} resolution. Each sample was scanned under the same conditions all of which gave identical spectra. At the end of this process there were 3 replicates for every RIL from which FTIR spectra were obtained. The average spectra of these three replicates for each individual were used in detailed data analysis and statistical analysis. Collections of spectra and data manipulations were carried out using Spectrum One software (Perkin-Elmer).

The band positions were measured using wavenumber corresponding to the center of weight. Wavenumber can be denoted as frequency since there is a linear relationship in between them. For area measurements Spectrum One software was used and the area under the band curve was measured. For the determination of the variations in the peak area and peak positions, each original spectrum was analyzed by using the same software. The same software was also used for other spectral analyses including baseline correction and normalization. The spectra were normalized with respect to specific bands just for visual demonstration of the spectral differences in the spectra.

2.4. Statistical Analysis

The frequency and area values of the average spectrum of each RIL were measured and then averaged to be expressed as ‘mean of frequency/intensity \pm standard deviation (SD). Resistant and Sensitive data were analyzed statistically using parametric t- test with the Minitab statistical Software Release 13.0 program. A ‘p’ value less than or equal to 0.05 was considered as statistically significant. The degree of significance was denoted as less than or equal to $p < 0.05^*$, $p < 0.01^{**}$, $p < 0.001^{***}$.

2.5. Principal Component Analysis (PCA)

Principal Component Analysis (PCA) is a multivariate statistical method which generates a new set of variables, called principal components. Each principal component is a linear combination of the original variables. All the principal components are orthogonal to each other, so there is no redundant information. The contributions from the original variables are represented as percentage for every principal component. PCA analysis was performed using Matlab (R2011a, The MathWorks, Massachusetts, USA). The programme uses the frequency and intensity values recorded at every 1 cm^{-1} intervals of the spectra of samples. Then, the PCA plots of the desired spectral regions were obtained. The principal components represent the variables at the spectral region under consideration.

CHAPTER 3

RESULTS

3.1. General FTIR Spectra and Band Assignment of Durum Wheat RIL Seeds

Figure 17 demonstrates the representative infrared spectra of stem rust resistant and sensitive groups in 4000-650 cm^{-1} region. Figure 18 shows the representative infrared spectra of yellow rust (stripe) resistant and sensitive groups in 4000-650 cm^{-1} region. The main bands were labeled in the figures and detailed band assignments based on this study and other studies cited in literature were given in Table 3.

As seen from Figures 17 and 18, there are some minor differences in the area and frequency values of the resistant and sensitive groups for stem and yellow rust diseases, but they are not very apparent.

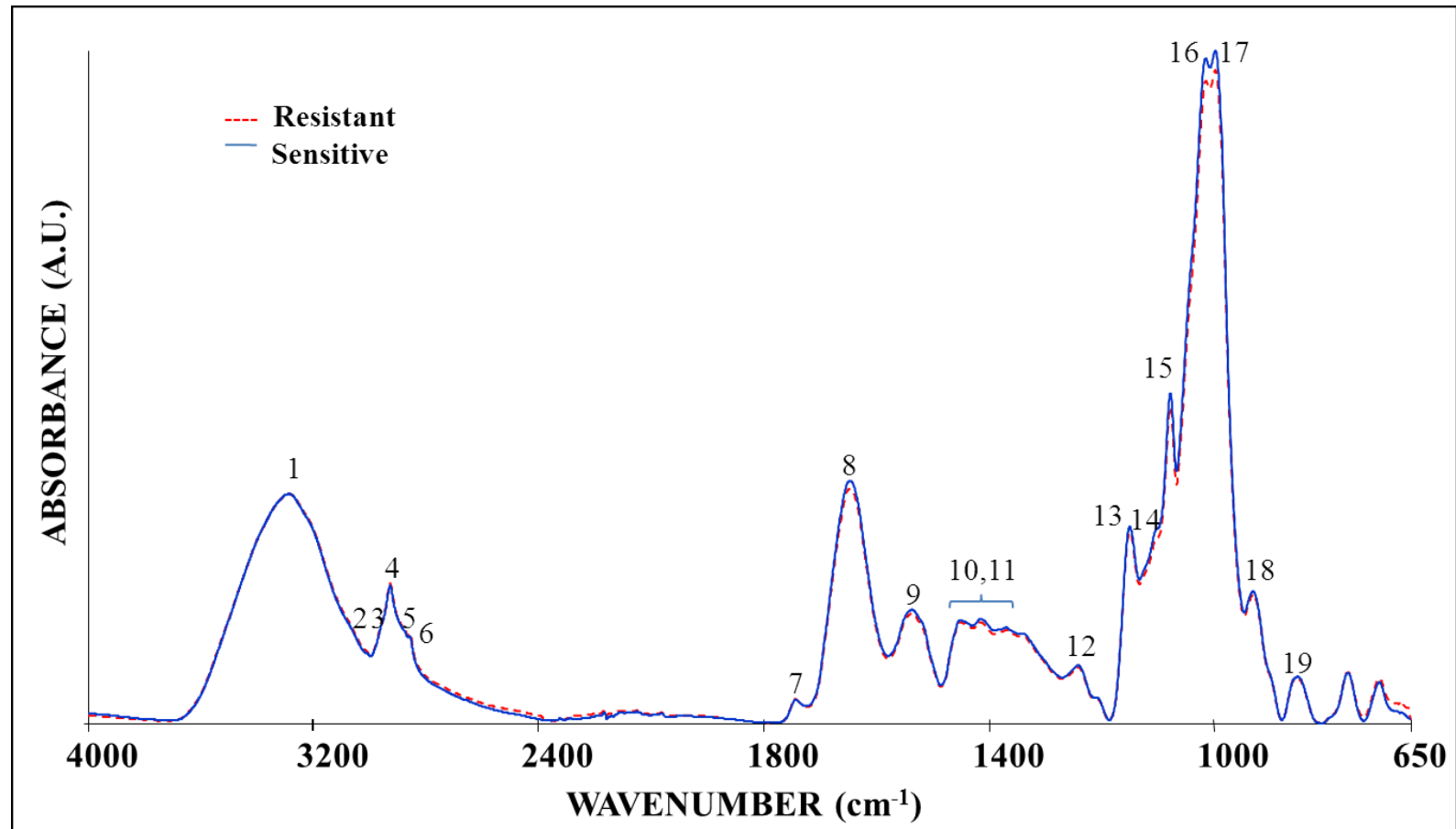


Figure 17. The representative infrared spectra of resistant and sensitive groups of stem rust disease in the region between 4000-650 cm⁻¹. (the spectra were normalized with respect to the Amide A mode at around 3300 cm⁻¹)

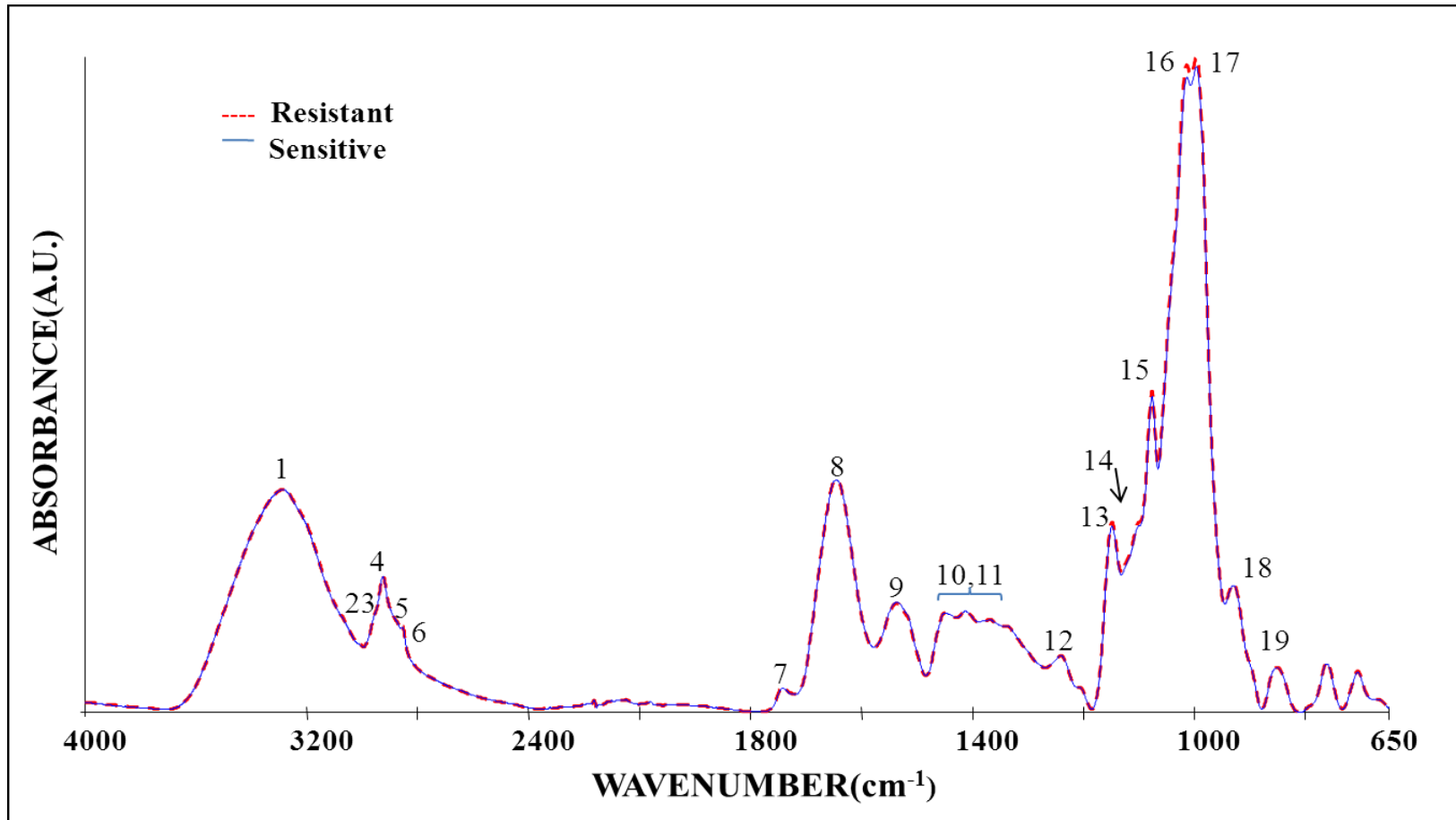


Figure 18. The representative infrared spectra of resistant and sensitive groups of yellow (stripe) rust disease in the region between 4000-650cm⁻¹. (The spectra were normalized with respect to the Amide A mode at around 3300 cm⁻¹)

Table 3. General band assignment of FT-IR spectrum of plants based on literature

Peak #	Wavenumber (cm-1)	Definition of Spectral Assignments
1	3380	O-H and N-H group stretching vibration:carbohydrates,protein
2	3012	C-H stretching of HC=CH groups in the fatty acids
3	2957	CH ₃ asymmetric stretching:mainly lipids with a little contribution from proteins, carbohydrates and nucleic acids
4	2922	CH ₂ asymmetric stretching:mainly lipids with a little contribution from proteins, carbohydrates and nucleic acids
5	2873	CH ₃ symmetric stretching:mainly proteins with a little contribution from lipids, carbohydrates and nucleic acids
6	2852	CH ₂ symmetric stretching: :mainly lipids with a little contribution from proteins, carbohydrates and nucleic acids
7	1733	Saturated ester C=O stretch: phospholipids, cholesterol esters, hemicellulose and pectin
8	1651	Amide I (protein C=O stretch): protein and pectin
9	1555	Amide II (C=N and N-H stretching): mainly proteins
10	1446	C-H: cell wall polysaccharides
11	1415	O-H bending: cell wall polysaccharides, alcohols and carboxylic acids
12	1235	Amide III (C=N and N-H stretching): mainly proteins
13	1145	Cellulose(β-1,4 glucan)
14	1101	Antisymmetric in-phase:pectic substances
15	1073	Rhamnogalactorunan. B-galactan
16	1035	OH and C-OH stretching: cell wall polysaccharides(arabinan)
17	931	Starch
18	850	Starch

3.2. Comparison of Stem Rust Resistant and Sensitive Durum Wheat Lines

FTIR spectral data were collected over the frequency range of 4000-650 cm^{-1} . In order to display the details of spectral changes, the analysis was performed in two distinct frequency ranges. The first range was 3700-2800 cm^{-1} and the second one was 1800-650 cm^{-1} . Since all resistant and sensitive spectra are overlapped, this reason, for the following discussions only one resistant and one sensitive spectrum will be chosen as a representative spectrum of each group.

Figure 19 shows the infrared spectra of stem rust resistant and sensitive lines in 3700-3000 cm^{-1} region. Figure 20 shows the infrared spectra of stem rust resistant and sensitive lines in 3020-2800 cm^{-1} region. As it could be seen from these figures resistant and sensitive spectra exhibit some minor differences in peak positions and peak areas.

Figure 21 demonstrates the infrared spectra of stem rust resistant and sensitive lines in 1800-650 cm^{-1} region. As it could be seen from the figure, the spectra exhibit some minor differences in area and frequency values in this region. These differences will be discussed more specifically.

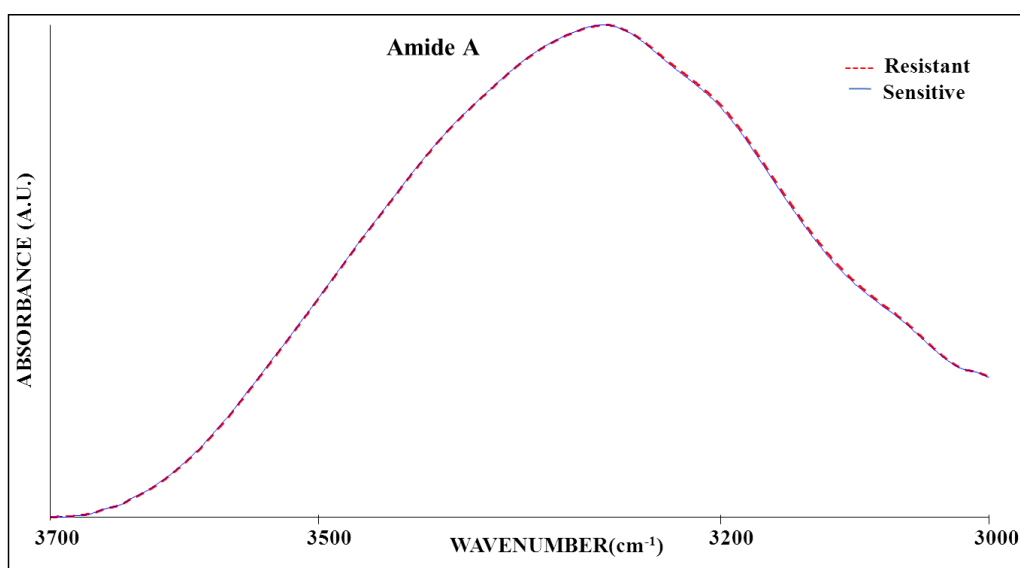


Figure 19. The representative infrared spectra of resistant and sensitive groups of stem rust disease in the region between 3700- 3000 cm⁻¹. (The spectra were normalized with respect to the CH₂ asymmetric stretching mode at 2926 cm⁻¹)

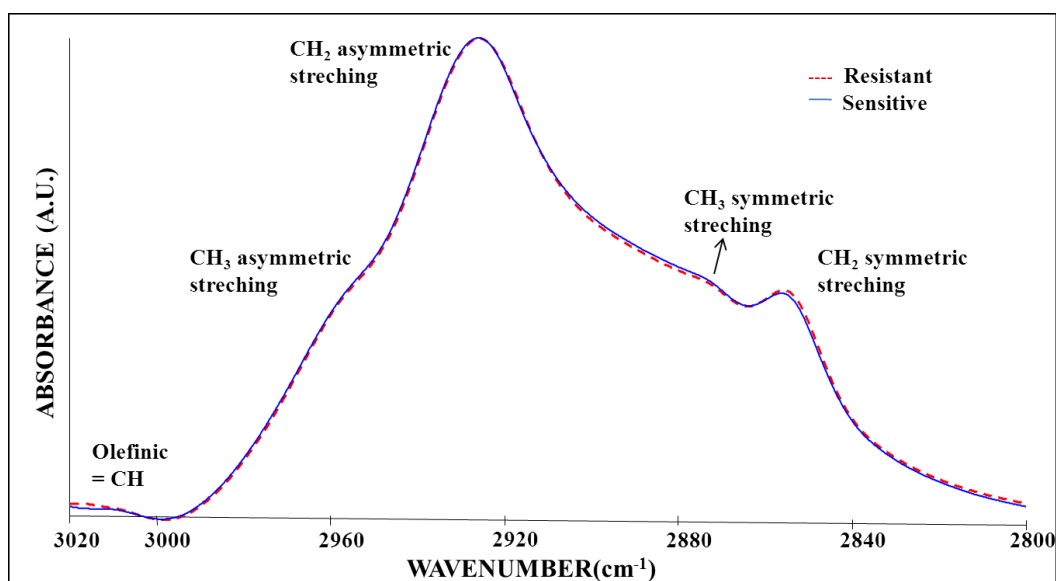


Figure 20. The representative infrared spectra of resistant and sensitive groups of stem rust disease in the region between 3020-2800 cm⁻¹. (The spectra were normalized with respect to the CH₂ asymmetric stretching mode at 2926 cm⁻¹).

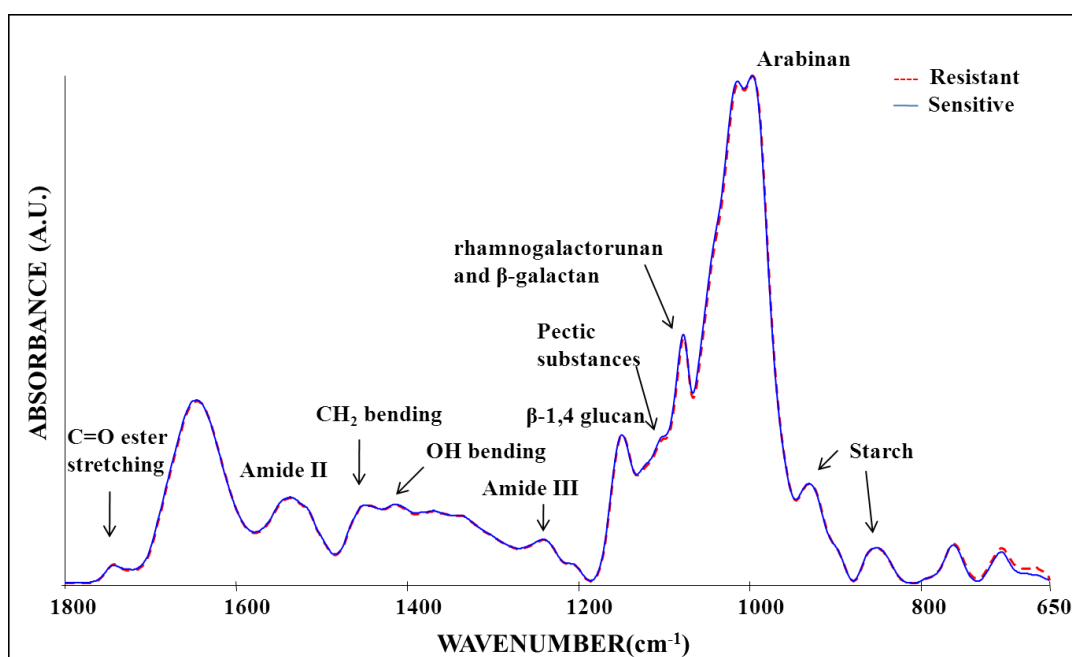


Figure 21. The representative infrared spectra of resistant and sensitive groups of stem rust disease in the region between 1800-650 cm^{-1} . (The spectra were normalized with respect to the Amide I at 1645 cm^{-1}).

On the basis of the spectra, PCA analysis was performed to see if resistance and sensitive RILs could be differentially grouped. The results were demonstrated in Figure 22. As seen in PCA plots based on different regions (3020-2800 cm^{-1} ; 2864-2840 cm^{-1} ; 3700-650 cm^{-1} ; 1273-1213 cm^{-1} ; 3020-2800, 1460-1445, 1772-1722 cm^{-1}), durum wheat lines were grouped in discrete clusters according to principal component 2. Although the resistant and sensitive lines were grouped in PCA plots, some of the samples are separated from the groups and are not clustered with neither sensitive nor resistant groups.

A.

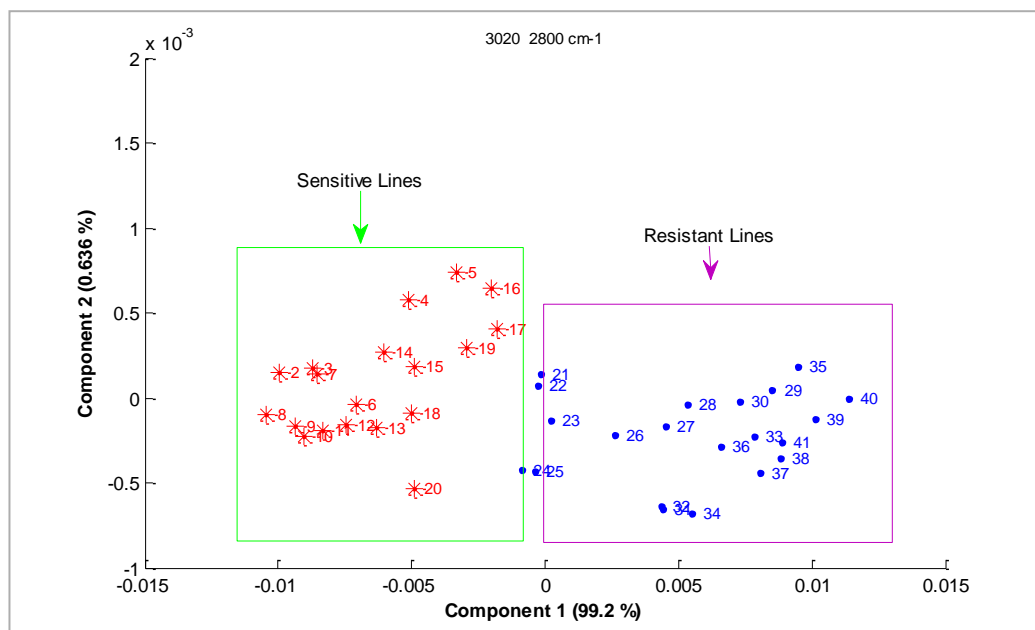
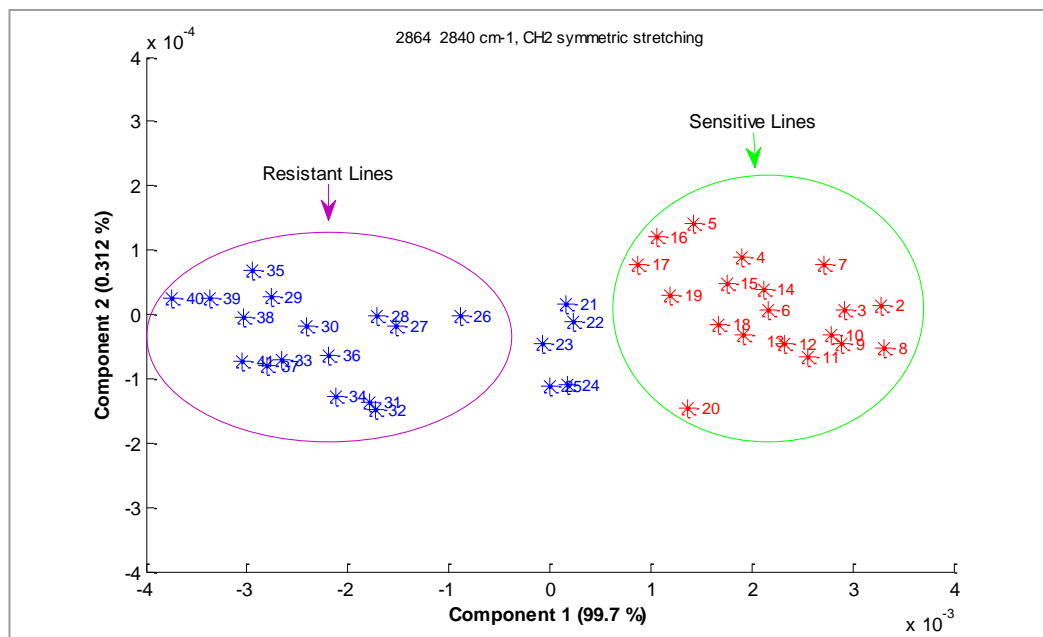


Figure 22. Classification of Resistant and Sensitive Lines to Stem Rust using PCA based on FTIR spectra. A. PCA plot based on 3020-2800 cm⁻¹ region. B. PCA plot based on CH₂ symmetric stretching mode (2864-2840cm⁻¹). C. PCA plot based on 3700-650 cm⁻¹ region. D. PCA plot based on Amide III band (1273-1213cm⁻¹). E. PCA plot based on C-H stretching region (3020-2800cm⁻¹), C=O stretching 1460-1445cm⁻¹) and CH₂ bending modes (1772-1722cm⁻¹). (*: Sensitive samples, •: Resistant samples).

B.



C.

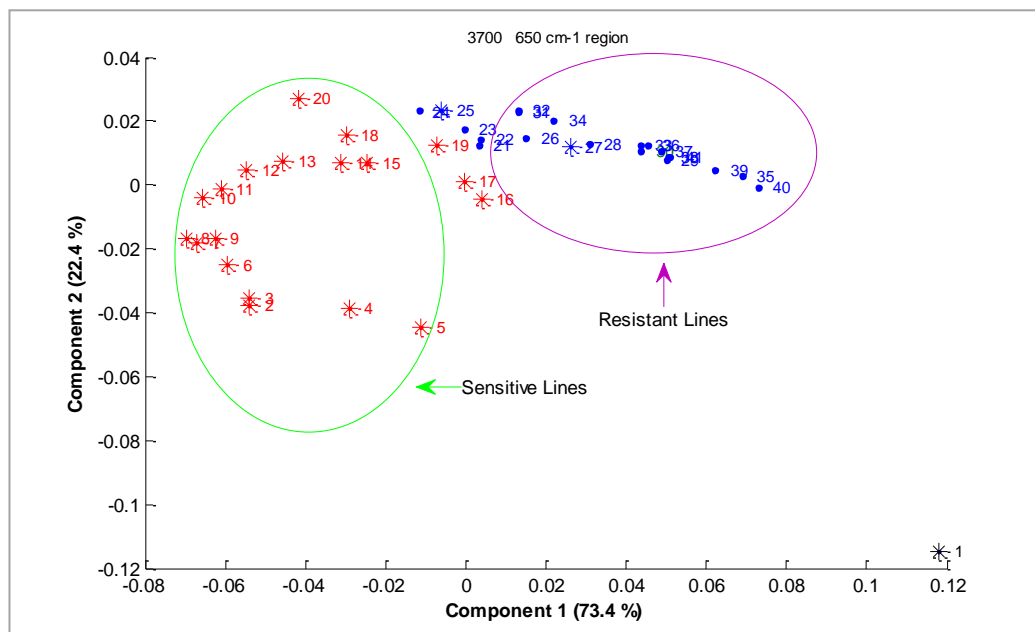
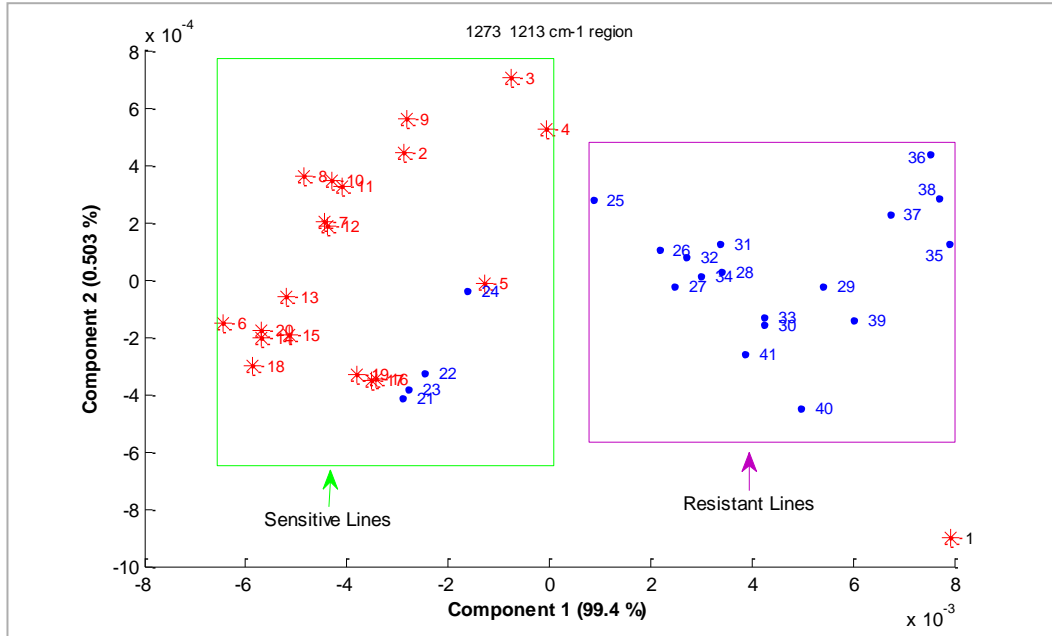


Figure 22. (continued)

D.



E.

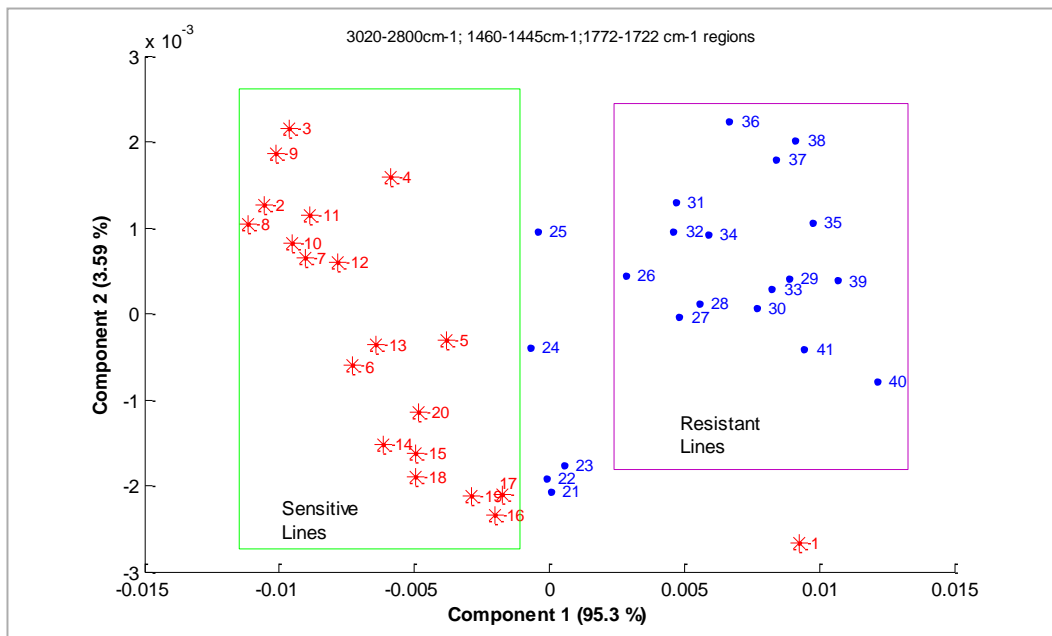


Figure 22. (continued)

3.2.1. Numerical Comparisons of the Bands of Stem Rust Resistant and Sensitive Durum Wheat Lines

In order to understand the differences between groups, the means and the standard deviations of the band areas and direction of the shifts with respect to sensitive group were obtained for resistant and sensitive groups. Resistant group-means were compared with those of sensitive group-means with the help of t-test and significance values were calculated. The results of changes in frequency values were given in Table 4, changes in band areas were given in Table 5.

Table 4. Numerical summary of the detailed differences in the band frequencies of resistant and sensitive spectra. The values are the mean \pm Standard Deviation for each sample. The degree of significance was denoted as $p < 0.05^*$, $p < 0.01^{**}$, $p < 0.001^{***}$.

Band No	BAND FREQUENCY	
	Stem Rust Resistant	Stem Rust Sensitive
1	3291.32 \pm 1.38↓	3291.60 \pm 1.56
2	3013.15 \pm 3.69↑	3011.50 \pm 3.29
3	2959.08 \pm 0.49↓	2959.30 \pm 0.70
4	2926,30 \pm 0,35↓	2926,50 \pm 0,41
5	2873,06 \pm 0,19↓	2873,08 \pm 0,33
6	2853,75 \pm 0,28↓	2853,92 \pm 0,52
7	1744.75 \pm 0.30↓	1744.90 \pm 0.59
8	1645.08 \pm 0.51↓	1645.19 \pm 0.51
9	1534.01 \pm 0.76↑	1533.75 \pm 1.67
10	1454.66 \pm 0.28↑	1454.49 \pm 0.25
11	1412.38 \pm 0.74 ^{**} ↑	1411.65 \pm 0.81
12	1240.20 \pm 0.27↓	1240.32 \pm 0.39
13	1147.68 \pm 0.27↑	1147.52 \pm 0.32
14	1104.43 \pm 0.07↓	1104.47 \pm 0.07
15	1077.55 \pm 0.11↑	1077.54 \pm 0.13
16	1017.97 \pm 0.26↓	1018.12 \pm 0.34
17	929.70 \pm 0.22↓	929.96 \pm 0.48
18	851.42 \pm 0.34↑	851.34 \pm 0.65

Table 5. Numerical summary of the detailed differences in the band areas of resistant and sensitive spectra. The values are the mean \pm Standard Deviation for each sample. The degree of significance was denoted as $p < 0.05^*$, $p < 0.01^{**}$, $p < 0.001^{***}$.

Band No	BAND AREA	
	Stem Rust Resistant	Stem Rust Sensitive
1	48.89 \pm 5.82 \uparrow	45.46 \pm 7.62
2	0.94 \pm 0.14* \uparrow	0.86 \pm 0.13
3	1.68 \pm 0.24 \uparrow	1.55 \pm 0.24
4	2.90 \pm 0.37 \uparrow	2.67 \pm 0.42
5	0.81 \pm 0.11 \uparrow	0.75 \pm 0.11
6	1.02 \pm 0.10* \uparrow	0.99 \pm 0.14
7	0.40 \pm 0.06 \uparrow	0.37 \pm 0.09
8	10.51 \pm 1.21 \uparrow	10.20 \pm 1.60
9	4.40 \pm 0.53*** \uparrow	2.98 \pm 1.56
10	0.81 \pm 0.08 \uparrow	0.78 \pm 0.11
11	3.71 \pm 0.35 \uparrow	3.58 \pm 0.52
12	1.45 \pm 0.11 \uparrow	1.41 \pm 0.18
13	3.22 \pm 0.31 \uparrow	3.10 \pm 0.44
14	1.89 \pm 0.18 \uparrow	1.85 \pm 0.25
15	4.38 \pm 0.41 \uparrow	4.29 \pm 0.57
16	15.59 \pm 1.56 \uparrow	15.23 \pm 2.17
17	2.42 \pm 0.24 \uparrow	2.33 \pm 0.35
18	0.80 \pm 0.07 \uparrow	0.77 \pm 0.11

3.2.2. Detailed Spectral Analysis

3.2.2.1. Comparison of Stem Rust Resistant and Sensitive Spectra in 3700-2800 cm^{-1} Region

As seen from Figures 19 and 20 the 3700-2800 cm^{-1} region contains several bands. The band centered at 3291 cm^{-1} (Amide A) corresponds to the OH and/or the NH stretching mode of proteins and carbohydrates. The band centered at 3012 cm^{-1} monitors stretching mode of the H-C=C-H vibrations. The other bands between 3050-2800 cm^{-1} are in the C-H region. These bands are centered at 2959 cm^{-1} , 2926 cm^{-1} , 2873 cm^{-1} and 2853 cm^{-1} , and they monitor both CH_3 and CH_2 asymmetrical, and both CH_3 and CH_2 symmetrical vibrations, respectively (Melin *et al.*, 2000; Chang and Tanaka, 2002; Çakmak *et al.*, 2003; Severcan *et al.*, 2003, Cakmak *et al.*, 2006).

As it can be seen from the Table 5 there is an increase in the area of Amide A band for resistant lines but this is insignificant. The frequency of the Amide A band shifted slightly to a lower value in resistant lines from $3291.60 \pm 1.56 \text{ cm}^{-1}$ to $3291.32 \pm 1.38 \text{ cm}^{-1}$, which was insignificant.

The area of the band located at 3012 cm^{-1} , which is due to the CH stretching mode of the HC=CH groups, can be used as a measure of unsaturation in the phospholipid acyl chains (Takahashi *et al.*, 1991; Melin *et al.*, 2000; Liu *et al.*, 2002; Severcan *et al.*, 2005). There was an increase in the area of this band for resistant lines ($p < 0.05^*$). The frequency of the band located at 3012 cm^{-1} shifted slightly to a higher value for resistant lines from $3011.50 \pm 3.29 \text{ cm}^{-1}$ to $3013.15 \pm 3.69 \text{ cm}^{-1}$, but this change was insignificant.

The CH_3 asymmetric (2959 cm^{-1}), the CH_2 asymmetric (2926 cm^{-1}), and the CH_2 symmetric (2853 cm^{-1}) stretching bands originate mainly from lipids, whereas the CH_3 (2873 cm^{-1}) symmetric stretching band originate mainly from proteins (Mantsch,

1984; Severcan *et al.* 1997; Severcan *et al.*, 2000; Severcan *et al.*, 2003, Cakmak *et al.*, 2006). For resistant lines there was a slight increase in the areas of the CH₃ symmetric stretching vibrations. The frequency of CH₃ asymmetric and symmetric bands in resistant group shifted to lower frequencies but these shifts are insignificant.

The CH₂ stretching vibrations depend on the degree of conformational disorder; therefore they can be used to monitor the average trans/gauche isomerization in the system (Mantsch *et al.*, 1984; Severcan, 1997; Bizeau *et al.*, 2000). Their band frequencies increase with the introduction of gauche conformers in the fatty acyl chains (Rana *et al.*, 1990; Schultz *et al.*, 1991; Melin *et al.*, 2000; Çakmak *et al.*, 2003; Cakmak *et al.*, 2006)

As seen in Table 5, the areas of the CH₂ asymmetric and symmetric stretching vibrations located at 2926 cm⁻¹ and 2853 cm⁻¹ respectively, increased in resistant lines. This increase is significant for the CH₂ symmetric stretching mode (p<0.05*). The frequency of CH₂ asymmetric stretching band shifted to a slightly lower frequency value in resistant lines from 2926.50 ± 0.41 cm⁻¹ to 2926.30 ± 0.35 cm⁻¹ and the frequency of the CH₂ symmetric stretching band shifted to a lower frequency value but these changes are not significant (Table 4).

The amount of proteins and lipids in the membranes is an important factor affecting the membrane structure and dynamics (Szalontai *et al.*, 2000). From the FTIR spectrum, lipid-to-protein ratio can be obtained by the ratio of the areas of the bands that stem from lipids and proteins (Table 6). As seen in Table 6, the ratio of the area of the CH₂ asymmetric stretching band to the area of the CH₃ symmetric stretching band which gives lipid-to-protein ratio is same in both resistant and sensitive groups. The lipid-to-protein ratio can also be calculated as the ratio of the sum of the areas of the CH₂ asymmetric and symmetric stretching bands to the area of the CH₃ symmetric stretching band which is lower in resistant group. Another value for lipid-to-protein ratio is the ratio of CH₂ symmetric and CH₃ symmetric stretching mode areas. On the contrary, this value is higher in resistant groups (p<0.05*).

Table 6. Numerical summary of the detailed differences in the lipid-to-protein ratios of stem rust resistant and sensitive spectra. The values are the mean \pm Standard Deviation for each sample. The degree of significance was denoted as $p < 0.05^*$, $p < 0.01^{**}$, $p < 0.001^{***}$.

Ratio of Peak Areas (lipid to protein)	Resistant	Sensitive
CH₂ Asym. / CH₃ Sym.	3,57 \pm 0,06	3,57 \pm 0,06
CH₂ Sym. / CH₃ Sym.	1,34 \pm 0,02* \uparrow	1,32 \pm 0,02
CH₂Asym.+ CH₂ Sym. / CH₃ sym.	4,90 \pm 0,07 \downarrow	4,98 \pm 0,35

3.2.2.2. Comparison of Stem Rust Resistant and Sensitive Spectra in 1800-650 cm⁻¹ Region

Figure 21 demonstrates the normalized infrared spectra of stem rust resistant and sensitive lines in 1800-650 cm⁻¹ region. 1800-650 cm⁻¹ frequency range, which is called as the fingerprint region, includes several bands that originate from the interfacial and head-group modes of the lipids and from the protein and carbohydrate vibrational modes (Mendelsohn & Mantsch, 1986).

The band centered at 1744 cm⁻¹ is mainly assigned to the >C=O ester stretching vibration represents ester-containing compounds in membrane lipids (cholesterol esters), cell wall pectin, and hemicellulose (Yang & Yeng, 2002; Melin *et al.*, 2000; Jamin *et al.*, 1998). There is a decrease in the frequency of this band in resistant group while an increase in band area is observed.

The bands at 1645 and 1533 cm^{-1} are attributed to the amide I and II vibrations of structural proteins. The band centered at 1645 cm^{-1} (amide I) corresponds to the C=O stretching and the C-N stretching (% 60) vibrational modes weakly coupled with the N-H bending (% 40) of the polypeptide and protein backbone and the band located at 1533 cm^{-1} (amide II) is assigned to the N-H bending (% 60) and the C-N stretching (% 40) modes of proteins (Melin *et al.*, 2000; Takahashi *et al.*, 1991; Wong *et al.*, 1991; Haris & Severcan, 1999; Çakmak *et al.*, 2003). The band areas of amide I and amide II bands increased in resistant lines but this increase is significant for only Amide II band ($p < 0.001^{***}$) (Table 5). There was a slight shift in the frequency of Amide I band to lower values from $1645.19 \pm 0.51 \text{ cm}^{-1}$ to $1645.08 \pm 0.51 \text{ cm}^{-1}$ (Table 4). For Amide II band there is a slight increase in frequency from 1533.75 ± 1.67 to $1534.01 \pm 0.76 \text{ cm}^{-1}$. As it was shown in Table 6, there was a narrowing in the bandwidths of both Amide I and Amide II bands for the resistant group but these changes are not significant.

An increase in the area of the band at 1454 cm^{-1} , which is assigned to the C-H group of carbohydrates (Dalvi *et al.*, 2000), is observed for resistant lines. As seen from Table 4, there was a shift to a higher value in the frequency of this band.

There is an increase in O-H bending band frequency in resistant lines from 1411.65 ± 0.81 to $1412.38 \pm 0.74 \text{ cm}^{-1}$ (Table 4). This band is assigned to cell wall polysaccharides, alcohols and carboxylic acids. In the area of this band no significant change is observed.

The band located at 1240 cm^{-1} is the result of Amide III vibrations, more specifically it originates from C=N and N-H stretching of mainly proteins. While a decrease is observed in band frequency, for area of this band there is a slight increase, which are both insignificant.

The band centered at 1147 cm^{-1} is assigned to be β -1,4 glucan units of Cellulose. The slight increases in both of its frequency (Table 4) and area (Table 5) are not

significant. As it can be seen from Table 4, the band located at 1104 cm^{-1} is assigned to pectic substances which are composed of high homogalacturonan content (Kacurokova *et al.*, 2000). The band at 1077 cm^{-1} can be specific for both rhamnogalactorunan and β -galactan (Bestard *et al.*, 2001).

3.3. Comparison of Yellow (Stripe) Rust Resistant and Sensitive Durum Wheat Lines

FTIR spectral data were collected over the frequency range of $4000\text{-}650\text{ cm}^{-1}$. In order to display the details of spectral changes, the analysis was performed in two distinct frequency ranges. The first range was $3700\text{-}2800\text{ cm}^{-1}$ and the second was $1800\text{-}650\text{ cm}^{-1}$. All resistant and sensitive spectra are overlapped. For this reason, for the following discussions only one resistant and one sensitive spectrum will be chosen as a representative spectrum.

Figure 23, figure 24 and figure 25 show the infrared spectra of yellow rust resistant and sensitive lines in $3700\text{-}3000\text{ cm}^{-1}$, $3020\text{-}2800\text{ cm}^{-1}$ and $1800\text{-}650\text{ cm}^{-1}$ region, respectively. As seen from these figures resistant and sensitive spectra exhibit some minor differences in peak positions, peak heights and widths in this region. These differences will be discussed in detail.

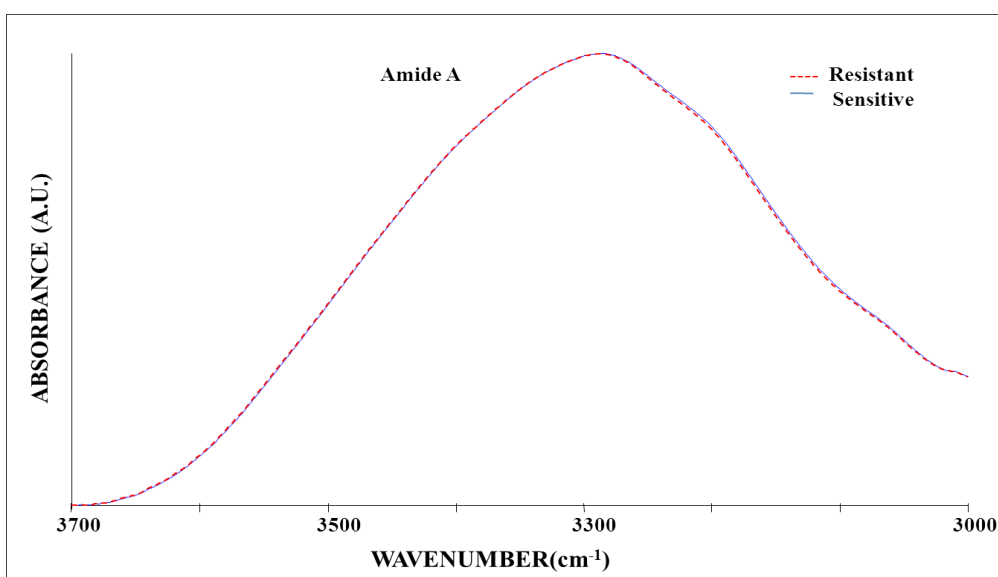


Figure 23. The representative infrared spectra of resistant and sensitive groups of yellow rust disease in the region between 3700- 3000 cm^{-1} . (The spectra were normalized with respect to the CH_2 asymmetric stretching mode at 2926 cm^{-1}).

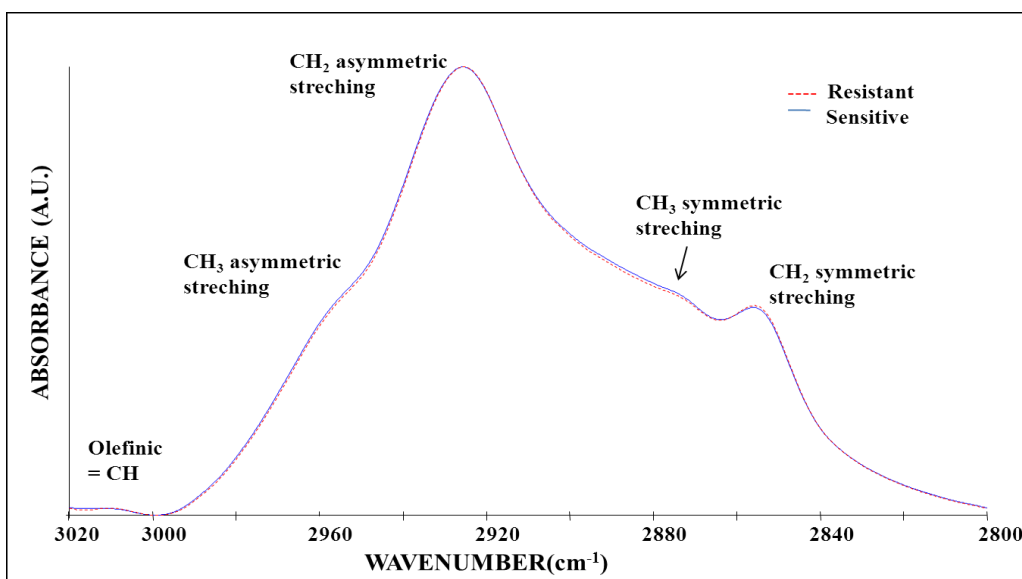


Figure 24. The representative infrared spectra of resistant and sensitive groups of yellow rust disease in the region between 3020-2800 cm^{-1} . (The spectra were normalized with respect to the CH_2 asymmetric stretching mode at 2926 cm^{-1}).

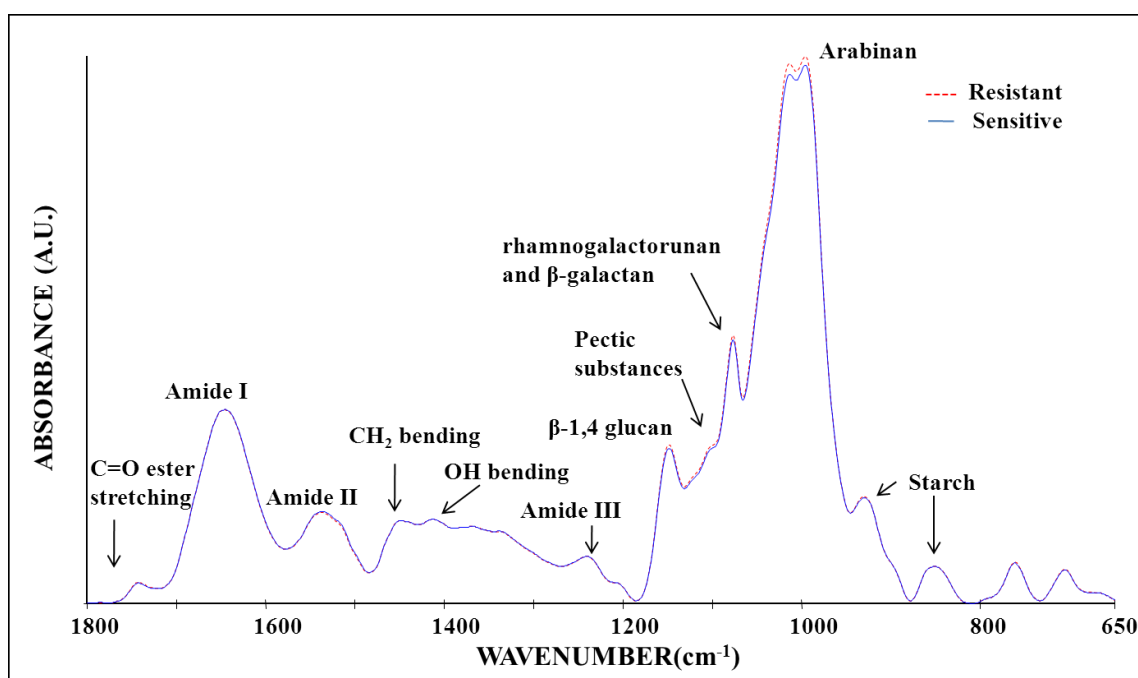
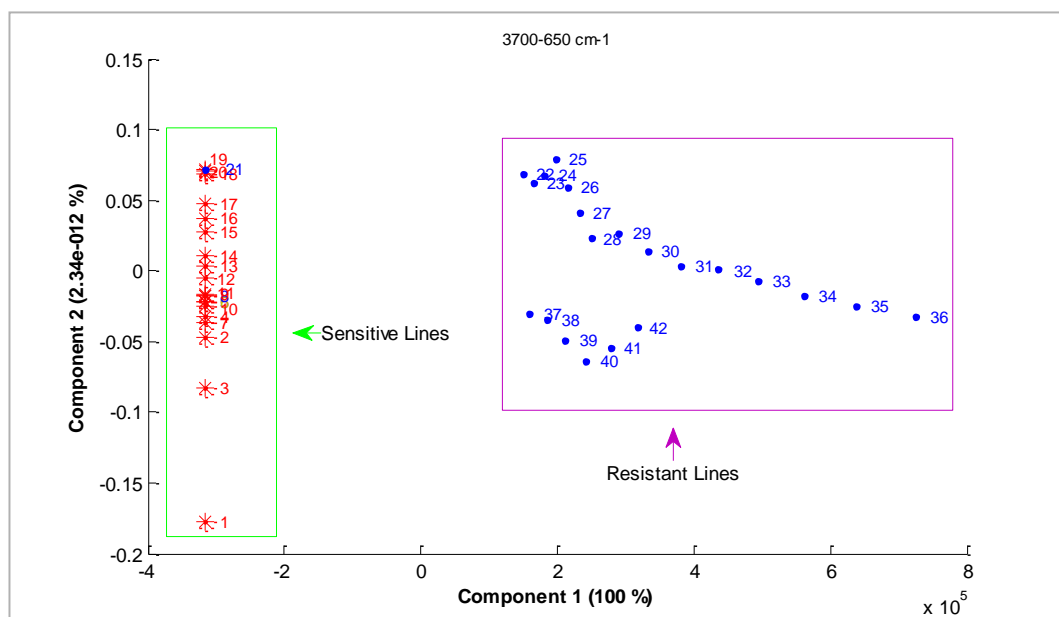


Figure 25. The representative infrared spectra of resistant and sensitive groups of yellow rust disease in the region between 1800-650 cm^{-1} . (The spectra were normalized with respect to the Amide I at 1645 cm^{-1}).

On the basis of the spectra, PCA analysis was performed for different spectral regions (3700-650 cm^{-1} ; 3700-3020 cm^{-1} ; 1272-1214 cm^{-1}) which were represented in Figure 26. Regarding 3700-650 cm^{-1} frequency range, Amide A and Amide III bands the durum wheat lines are clustered as resistant and sensitive groups according to principal component 2. . Although the resistant and sensitive lines were grouped in PCA plots, four of the samples are separated from the groups and are not clustered with either sensitive or resistant group according to Amide A.

A.



B.

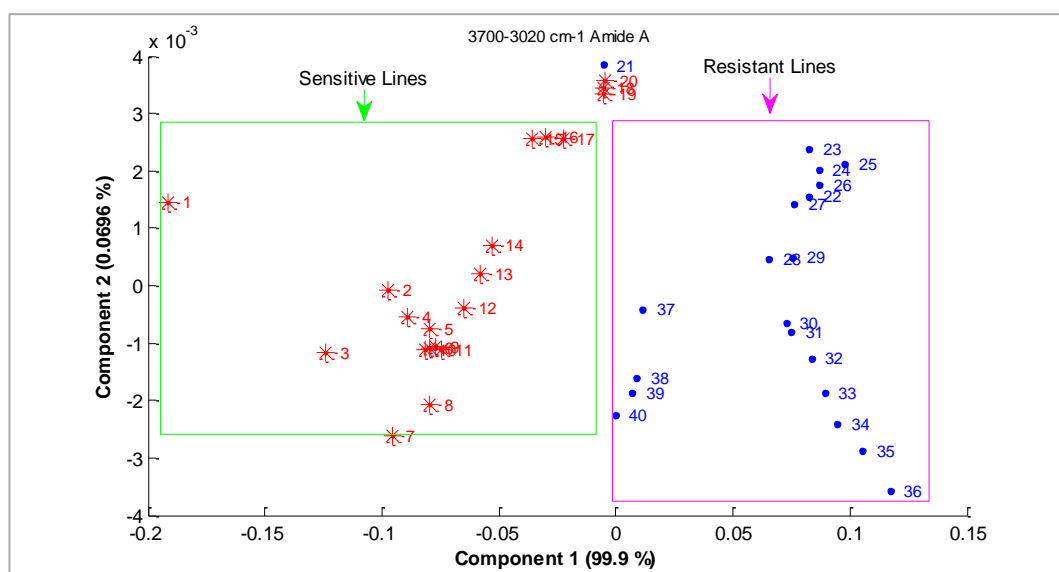


Figure 26. Classification of Resistant and Sensitive Lines to Yellow Rust using PCA based on FTIR spectra. A. PCA plot based on 3700-650 cm^{-1} region B. PCA plot based on Amide A band (3700-3020 cm^{-1}) C. PCA plot based on Amide III band (1272-1214 cm^{-1}) (*: Sensitive samples, •: Resistant samples).

C.

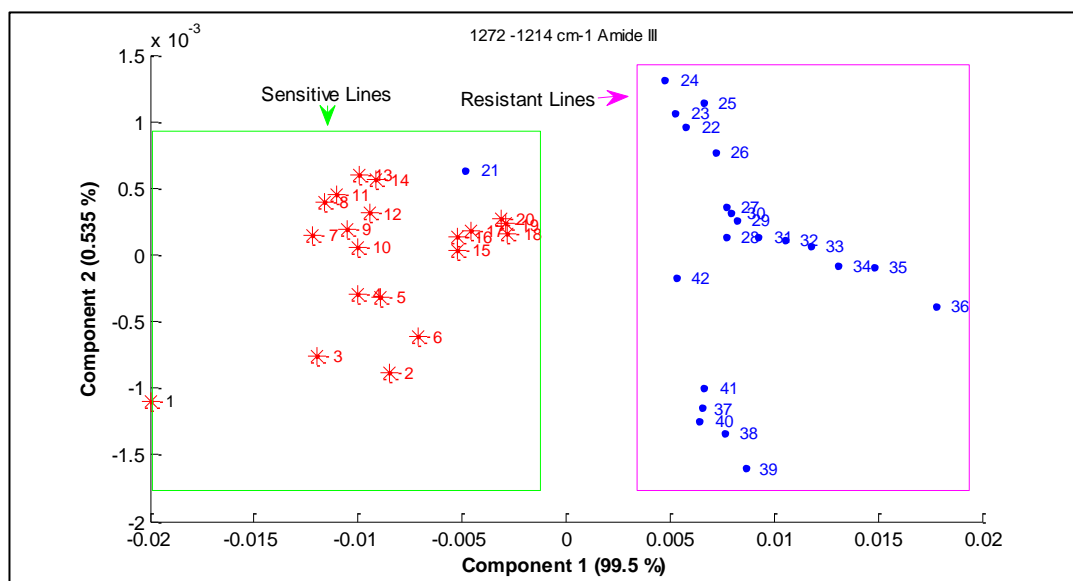


Figure 26. (continued)

3.3.1. Numerical Comparisons of the Bands of Yellow Rust Resistant and Sensitive Durum Wheat Lines

In order to understand spectral differences between resistant and sensitive groups, the means and the standard deviations of the band areas and direction of the shifts with respect to sensitive group were obtained for resistant and sensitive groups. Resistant group means were compared with those of sensitive group means with the help of t-test and significance values were calculated. The results of changes in frequency values were given in Table 7 and changes in band areas were given in Table 8.

Table 7. Numerical summary of the detailed differences in the band frequencies of resistant and sensitive spectra. The values are the mean \pm Standard Deviation for each sample. The degree of significance was denoted as $p < 0.05^*$, $p < 0.01^{**}$, $p < 0.001^{***}$.

Band No	BAND FREQUENCY	
	Yellow Rust Resistant	Yellow Rust Sensitive
1	3291.84 \pm 1.77* \downarrow	3292.93 \pm 1.12
2	3011.95 \pm 3.66 \uparrow	3011.39 \pm 3.70
3	2959.04 \pm 0.84 \downarrow	2959.06 \pm 0.43
4	2926.00 \pm 0.20* \downarrow	2926.17 \pm 0.24
5	2873.19 \pm 0.14 \downarrow	2873.28 \pm 0.29
6	2853.54 \pm 0.11 \uparrow	2853.49 \pm 0.13
7	1744.71 \pm 0.38 \downarrow	1744.88 \pm 0.42
8	1645.05 \pm 0.48 \uparrow	1644.90 \pm 0.59
9	1534.146 \pm 0.88 \uparrow	1533.55 \pm 1.03
10	1454.52 \pm 0.21 \downarrow	1454.63 \pm 0.24
11	1411.30 \pm 0.52 \downarrow	1411.31 \pm 0.72
12	1240.31 \pm 0.25 \uparrow	1240.27 \pm 0.40
13	1147.85 \pm 0.18 \uparrow	1147.68 \pm 0.36
14	1104.51 \pm 0.07 \uparrow	1104.50 \pm 0.09
15	1077.45 \pm 0.13 \uparrow	1077.36 \pm 0.18
16	1017.95 \pm 0.24 \uparrow	1017.79 \pm 0.24
17	929.93 \pm 0.43 \uparrow	929.82 \pm 0,20
18	851.26 \pm 0.57 \downarrow	851.55 \pm 0,81

Table 8. Numerical summary of the detailed differences in the band areas of resistant and sensitive spectra. The values are the mean \pm Standard Deviation for each sample. The degree of significance was denoted as $p < 0.05^*$, $p < 0.01^{**}$, $p < 0.001^{***}$.

Band No	BAND AREA	
	Yellow Rust Resistant	Yellow Rust Sensitive
1	46.43 \pm 5.02↓	51.87 \pm 18.22
2	0.80 \pm 0.09↓	0.90 \pm 0.33
3	2.29 \pm 0.23↓	2.58 \pm 0.94
4	3.02 \pm 0.31↓	3.36 \pm 1.23
5	0.77 \pm 0.07↓	0.86 \pm 0.31
6	1.02 \pm 0.10↓	1.14 \pm 0.42
7	0.29 \pm 0.05↓	0.30 \pm 0.14
8	10.08 \pm 1.12↓	11.30 \pm 4.30
9	4.18 \pm 0.47↓	4.75 \pm 1.90
10	1.53 \pm 0.14↓	1.71 \pm 0.61
11	2.11 \pm 0.20↓	2.36 \pm 0.84
12	1.40 \pm 0.12↓	1.57 \pm 0.56
13	3.17 \pm 0.31↓	3.47 \pm 1.13
14	3.10 \pm 0.31↓	3.40 \pm 1.14
15	4.63 \pm 0.46↓	5.10 \pm 1.72
16	16.01 \pm 1.72↓	17.58 \pm 5.76
17	2.27 \pm 0.23↓	2.53 \pm 0.85
18	0.77 \pm 0.07↓	0.85 \pm 0.28

3.3.2. Detailed Spectral Analysis

3.3.2.1. Comparison of Yellow Rust Resistant and Sensitive Spectra in 3700-2800 cm^{-1} Region

As seen from Figures 23 and 24, the 3700-2800 cm^{-1} region contains several bands whose band assignments were discussed in previous results part. As it can be seen from the Table 8 there is a decrease in the area of Amide A band for resistant lines but this is not significant. The frequency of the Amide A band shifted slightly to a lower value in resistant lines from $3292.93 \pm 1.12 \text{ cm}^{-1}$ to $3291.84 \pm 1.77 \text{ cm}^{-1}$ ($p < 0.05^*$) (Table 7).

There was a slight increase in the frequency and a slight decrease in the area of olefinic band at 3011 cm^{-1} for resistant lines but these changes are not significant.

For resistant lines there was a slight decrease in the frequencies of the CH_3 asymmetric and symmetric stretching vibrations as shown in table 7. The areas of CH_3 asymmetric and symmetric bands in resistant group also shifted to lower values but these shifts are insignificant (Table 8).

As seen in Table 8, the areas of the CH_2 asymmetric and symmetric stretching vibrations (2926 cm^{-1} and 2853 cm^{-1} respectively), decreased in resistant lines. The frequency of CH_2 asymmetric stretching band shifted to a slightly lower frequency value in resistant lines from $2926.17 \pm 0.24 \text{ cm}^{-1}$ to $2926.0 \pm 0.20 \text{ cm}^{-1}$ ($p < 0.05^*$) (Table 7). The frequency of the CH_2 symmetric stretching band shifted to a higher frequency value but this change is not significant.

From the FTIR spectrum, a precise lipid-to-protein ratio can be derived by calculating the ratio of the areas of the bands arising from lipids and proteins. As it is seen from Table 9, the ratio of the area of the CH_2 asymmetric stretching band to the area of the CH_3 symmetric stretching band which gives lipid-to-protein ratio is lower

in resistant ones. Also the lipid-to-protein ratio could be calculated as the ratio of the sum of the areas of the CH₂ asymmetric and symmetric stretching bands to the area of the CH₃ symmetric stretching band, which is higher in resistant group. The last value for lipid-to-protein ratio is calculated as the ratio of CH₂ symmetric and CH₃ symmetric stretching modes which is slightly higher in resistant group.

Table 9. Numerical summary of the detailed differences in the lipid-to-protein ratios of yellow rust resistant and sensitive spectra. The values are the mean \pm Standard Deviation for each sample. The degree of significance was denoted as $p < 0.05^*$, $p < 0.01^{**}$, $p < 0.001^{***}$.

Ratio of Peak Areas (lipid to protein)	Resistant	Sensitive
CH₂ Asym. / CH₃ Sym.	3,92 \pm 0,05 \downarrow	3,95 \pm 0,21
CH₂ Sym. / CH₃ Sym.	1,33 \pm 0,02 \uparrow	1,32 \pm 0,02
CH₂ Asym.+ CH₂ Sym. / CH₃ sym.	5,32 \pm 0,31 \uparrow	5,22 \pm 0,07

3.3.2.2. Comparison of Yellow Rust Resistant and Sensitive Spectra in 1800-650 cm⁻¹ Region

The second frequency range under consideration was that of 1800-650 cm⁻¹ region. The 1800-650 cm⁻¹ frequency range, which is called as the fingerprint region, includes several bands that originate from the interfacial and head-group modes of the lipids and from the protein and carbohydrate vibrational modes (Mendelsohn &

Mantsch, 1986). Figure 25 demonstrates the normalized infrared spectra of yellow rust resistant and sensitive lines in 1800-650 cm^{-1} region.

There was a decrease in the frequency of $>\text{C}=\text{O}$ ester stretching vibration band, which is centered at 1744 cm^{-1} , in resistant group together with a decrease in band area (Tables 7 & 8). These changes were not significant.

The band areas of amide I and amide II bands decreased in resistant lines but this increase was not significant (Table 8). There was a slight shift in the frequency of Amide I band to higher values from $1644.90 \pm 0.59 \text{ cm}^{-1}$ to $1645.05 \pm 0.48 \text{ cm}^{-1}$. For Amide II band there was a slight increase in frequency from 1533.55 ± 1.03 to 1534.14 ± 0.88 (Table 7).

A decrease in the area of the band at 1454 cm^{-1} , which is assigned to the CH_2 bending mode of protein and lipids (Manoharan *et al.*, 1993; Çakmak *et al.*, 2003), was observed for resistant lines. As seen from Table 7, there was a shift to a lower value in the frequency of this band.

There was a decrease in O-H bending band frequency in resistant lines from 1411.31 ± 0.72 to $1411.30 \pm 0.52 \text{ cm}^{-1}$ (Table 7). In the area of this band there is a slight decrease but not significant.

The band located at 1240 cm^{-1} is the result of Amide III vibrations. While an increase was observed in band frequency, for area of this band there was a slight decrease, which are both insignificant (Tables 7 & 8).

The band centered at 1147 cm^{-1} is assigned to be β -1,4 glucan units of cellulose. The slight increases in frequency and decrease in area of this band were not significant (Tables 7 & 8).

As it can be seen from Table 7 the band located at 1104 cm^{-1} is assigned to pectic substances, which are composed of high homogalacturonan content (Kacurokova *et al.*, 2000). The band at 1077 cm^{-1} is specific for both rhamnogalacturonan and β -galactan (Bestard *et al.*, 2001). The changes in frequency and area values of these bands were not significant.

CHAPTER 4

DISCUSSION

As it was explained in detail in the introduction chapter, fungal diseases of plants are among the catastrophic diseases of plants and rust diseases are the most devastating fungal diseases of wheat. Stem rust and yellow rust epidemics has resulted in great yield losses all over the world. The races of pathogenic rust fungi that are capable of overcoming resistance genes of wheat species has been demonstrated for these rust diseases. Researches have been directed to obtain durable resistance to these rust diseases. The breeding strategies for obtaining resistant cultivars take long time and need significant efforts. The identification and discrimination of the resistant cultivars are crucial to prevent these devastating diseases.

Hence, the present study investigates the characterization of resistant and sensitive durum wheat lines to fungal diseases stem and yellow rusts by ATR-FTIR Spectroscopy. The differences in frequency and area values of resistance and sensitive groups were examined.

4.1. Discussion on Resistant and Sensitive RILs to Stem Rust Disease

In PCA, the samples were separately grouped as resistant and sensitive. For the full range of the spectra ($3700-650\text{ cm}^{-1}$) except for the 8 resistant samples, the sensitive and resistant groups were clustered together according to the principal component 1 which explains 73.4 % of the variables. For amide III band ($1213-1273\text{ cm}^{-1}$ region) resistant and sensitive lines were clustered according to principal component 1 with 99.4 % although there were 4 resistant samples in the sensitive group. The C-H stretching region ($3020-2800\text{ cm}^{-1}$) is the one that gave the most significant result for PCA analysis. The resistant and sensitive groups were clustered according to the

principal component 1 which reflects 99.2 % of the variables. Thus, Principal Component analysis can be used in discriminating the resistant and sensitive groups of stem rust disease.

In infrared spectroscopy, the signal intensity, more accurately the band areas in absorption spectra give information about the concentration of related functional groups (Freifelder, 1982; Toyran & Severcan, 2003; Toyran *et al.*, 2004). There observed significant changes for olefinic, CH₂ symmetric stretching, Amide II and OH bending bands for stem rust disease.

As seen in Table 5, there was a significant increase in the area of the olefinic (3011cm⁻¹) band. The intensity of olefinic band can be used as a measure of unsaturation in the acyl chains (Takahashi *et al.*, 1991, Liu *et al.*, 2002; Severcan *et al.*, 2005). The increase in area of this band indicates an increase in the population of unsaturation in acyl chains of lipid molecules. This increase in unsaturation state might indicate the high amount of unsaturated lipids or decrease in end products of lipid peroxidation (Kinder *et al.*, 1997). Actually oxidative processes occur in hypersensitive reaction in wheat-rust interactions after infection. An increase in lipid peroxidation has been shown in infected plants (Abdou *et al.*, 1993). Thus, it is expected to have decrease in lipid peroxidation products since the infection may be aborted by means of necrosis in resistant lines of wheat.

There was also a significant increase in the area of CH₂ symmetric stretching vibration. This increase may be a result of increase in lipid content of resistant group. The band centered at 1534 cm⁻¹ is Amide II. As seen in Table 5, there was a significant increase in the area of amide II band in resistant lines of durum wheat to stem rust disease indicating an increase in total protein content of the resistant group. According to this result, there may be an increase in protein content in resistant line seeds compared to sensitive ones. The increases in lipid and protein contents of the resistant group might be related to the response mechanisms of the host wheat plant to the fungal pathogen. It was shown that some leaf rust resistant genotypes and the

resistant crosses of *Triticum aestivum* had thicker epidermis and leaf lamina and more number of epidermal cells than the sensitive ones (Gelalcha & Hanchinal, 2003). There may be structural differences also in seeds of wheat so that the protein and lipid contents are higher for resistant lines.

The band centered at 1412 cm^{-1} is due to the O–H bending vibration of alcohols and carboxylic acids (Dalvi *et al.*, 2000). There was a significant shift for frequency of this band to higher values. This may be related to the lignification process. Lignification has been proposed to be a response mechanism in fungal infections of plants (Hijwegen, 1963). It was shown that induced lignification is an important mechanism in disease resistance (Vance *et al.*, 1980; Ride, 1983). Lignin is a complex compound which may include carboxylic acids and alcohols in its structure. It crosslinks with the cell wall components (Liyama *et al.*, 1994) and take role in cell wall strengtening. Therefore, in resistant lines, there may be an increase in lignin production, thus, an increase in carboxylic acids and alcohols.

4.2. Discussion on Resistant and Sensitive RILs to Yellow Rust Disease

In PCA (Figure 26), the samples were grouped as resistant and sensitive for 3700-650 cm^{-1} region, Amide A and Amide III bands. For 3700-650 cm^{-1} region the groups were successfully separated according to the principal component 2 representing 100 % of the variables. For Amide A band the sensitive and resistant lines were grouped according to principal component 2 representing 99.9 % of the variables, but four of the samples were not clustered in these groups. For Amide III band the groups were clustered according to principal component 2 explaining 99.5 % of the variables except one resistant sample which is seen in sensitive group. Thus, Principal Component analysis can be used for discriminating these two groups.

There observed two significant changes for resistant group to the yellow rust disease. For Amide A band (3291 cm^{-1}) there was a significant shift in the frequency to a lower value. This shift may suggest an increase in hydrogen bonding (Krimm & Bandekar, 1986). The increase in hydrogen bonding could be related with the stability of proteins since hydrogen bonds are important in secondary and tertiary structure of proteins. Thus, it can be concluded that resistant lines have more stabilized proteins in their seed structures. This may be related with the sensing or response mechanisms of the disease since receptors and enzymes are all proteins.

In Figure 25, the C-H region ($3020\text{-}2800\text{ cm}^{-1}$) is seen and contains absorptions arising from the C-H stretching vibrations. As seen in Table 8, there is a significant decrease in the area of CH_2 asymmetric stretching (2926cm^{-1}) band.

CH_2 asymmetric stretching band is correlated with the order/disorder state of membrane lipids. It is known that the increase in band frequency of CH_2 asymmetric stretching band is correlated with the introduction of gauche conformers into the fatty acyl chains in membrane structure (Melin *et al.*, 2000; Cakmak *et al.*, 2003; Toyran & Severcan, 2003). The results showed that the CH_2 asymmetric stretching band frequency was significantly lower for resistant lines. The lower frequency for CH_2 asymmetric stretching mode implies a more ordered membrane structure because it was composed of less gauche conformers but more trans conformers in the fatty acyl chains of membrane phospholipids. This can be again explained by the fact that the pathogen and the host interacts at membrane which aids in sensing and response mechanisms. Since, it was shown that membrane order and phospholipid structure may be related to the function and the activities of proteins in membrane (Poon *et al.*, 1981; Carruthers & Melchior, 1988; Yeagle, 1989). Thus, it can be concluded that the protein activities of resistant lines may be affected by the membrane order, which may further affect the resistance mechanisms to the disease.

CHAPTER 5

CONCLUSION

The results of the present study indicated that RILs of durum wheat used in this study, which of some are resistant to the particular rust disease and some are sensitive, showed some spectral alterations, but most of which are not significant. The observed changes in infrared spectra of resistant and sensitive durum wheat seeds were reported in this study for the first time.

In PCA, successful results were obtained. For stem rust disease, 3700-650 cm^{-1} , amide III band (1213-1273 cm^{-1} region) and C-H stretching region (3020-2800 cm^{-1}) demonstrated significant results to discriminate resistant lines from sensitive ones. For yellow rust disease, 3700-650 cm^{-1} region, Amide A and Amide III bands showed significant results in PCA analysis. There are some samples that were not grouped in either resistant or sensitive clusters. The reason for these exceptions may be the uncertainties in identification process of the durum wheat lines as resistant and sensitive. To a particular fungal disease, the reactions of lines to the diseases were evaluated according to a scale by the observations of the disease symptoms present on the plant. There may be ascertainment errors while observing these disease symptoms. In addition there were durum wheat lines that were classified in conversion to coefficient of infection values as MR (Moderately Resistant), MS (Moderately Sensitive), MR-MS or MS-MR. Due to the scarcity of samples that are completely resistant or completely sensitive, the lines, that are MR or MS, must have been used in this study. This situation might have affected the results in an inaccurate manner. Yet, the Principal Component Analysis provided substantial discriminating power in classification of the resistant and sensitive lines of durum wheat to both rust diseases.

For stem rust disease, resistant durum wheat lines had a significant increase in the population of unsaturation in acyl chains of lipid molecules, an increase in lipid and in total protein content and also an increase in carboxylic acids and alcohols. For yellow rust disease, resistant lines had a significant increase in hydrogen bonding and they had also a more ordered membrane structure. These results may result from the differences in resistance mechanisms, in which different sensing and response pathways observed.

The results given in this study showed the differences in infrared spectra of resistant and sensitive RILs to stem rust and yellow rust diseases. In addition, the results demonstrated the discrimination of resistant lines from the sensitive ones by using PCA. However, further research is necessary to analyze the molecular differences at different developmental stages of both resistant and sensitive infected plants in order to support the results of this study.

REFERENCES

- Abdou E., Galal A., Barna B. (1993). Changes in lipid peroxidation, superoxide dismutase, peroxidase and lipoxigenase enzyme activities in plant–pathogen interaction. In: Mozsik G, Emerit I, Fehe`r J, Matkovics B, Vincze A editors. Oxygen free radicals and scavengers in the natural sciences. Akade`mia Kiado: Budapest : 29–33.
- Almansouri M., Kinet J-M., Lutts S. (2001). Effect of salt and osmotic stresses on germination in durum wheat (*Triticum durum* Desf.). *Plant and Soil*, 231: 243–254.
- Arrondo, J.R., Muga, A., Castresa, J., and Goni, R. M. (1993). Quantative Studies of the Structure of Proteins in Solution by Fourier Transfrom Infrared Spectroscopy, *Prog Biophys Mol Biol.*, 59 (1): 23–56.
- Ayliffe M., Singh R. and Lagudah E. (2008). Durable resistance to wheat stem rust needed. *Current Opinion in Plant Biology*, 11: 187-192.
- Beharav A., Golan G., Levy A. (1997). Evaluation and variation in response to infection with *Puccinia striiformis* and *Puccinia recondita* of local wheat landraces. *Euphytica*, 94: 287–293.
- Bestard M.J., Sanjuan N., Rosselló C., Mulet A. and Femenia A. (2001). Effect of storage temperature on the cell wall components of broccoli (*Brassica oleracea* L. var. *Italica*) plant tissues during rehydration. *J. Food Eng.*, 48: 317–323.
- Bizeau, M.E., Salano, J.M., and Jeffrey, R. (2000). Menhaden oil feeding increases lypolysis without changing plasma membrane order in isolated rat adipocytes. *Nutrition Research*, 20 (11): 1633-1644.

Blum A., Golan G., Mayer J., Sinmena B., Shpiler L., and Burra J. (1989). The drought response of landraces of wheat from the northern Negev Desert in Israel. *Euphytica* 43: 87–96.

Bourdon S., Laggoun-Defarge F., Disnar J. R., Maman O., Guillet B., Derenne S., and Largeau C. (2000). Organic matter sources and early diagenetic degradation in a tropical peaty marsh. *Organic Geochem.*, 31: 421.

Cakmak G., Togan I., Uguz C., and Severcan F. (2003). FT-IR spectroscopic analysis of rainbow trout liver exposed to nonylphenol. *Appl. Spectrosc.*, 57: 835.

Cakmak, G., Togan, I., Severcan, F. (2006). 17-Estradiol induced compositional, structural and functional changes in rainbow trout liver, revealed by FT-IR spectroscopy: A comparative study with nonylphenol, *Aquatic Toxicology*, 77: 53–63.

Campbell, J. D., and Dwek, R. A. (1984). *Biological Spectroscopy*, Chapters 3, 4. Edited by: Elias, P. The Benjamin/Cummings Publishing Company, Inc.

Canlıhos, Y., Yagbasanlar, T., Kurt, S., Toklu, F. (1997). Cukurova bölgesinde bazı önemli buğday cesit ve hatlarının sarı pas ve septoria yaprak lekesi hastalıklarına karşı reaksiyonları. *CU. ZF Dergisi*, 12 (3): 89–98.

Carruthers A. And Melchior D., L. (1988). Effects of lipid environment on membrane transport: The Human Erythrocyte Sugar Transport Protein/Lipid Bilayer System. *Ann. Rev. Physiol.*, 50: 257-271.

Cereal Rusts and Powdery Mildews Conference. (1996). Lunteren, Netherlands. *Edited by* G.H.J. Kema, R.E. Nike, and R.A. Damen. European and Mediterranean Cereal Rust Foundation, Wageningen, Netherlands. *Cereal Rusts and Powdery Mildews Bulletin*, 24(Suppl.): 101–104.

Cetin, L., Dusunceli, F., Albustan, S. (1998). Bazi kislik ekmeklik ve makarnalik bugday örneklerinde pas (*Puccinia* spp.) hastaliklarına dayanikli genotiplerin Ankara kosullarında belirlenmesi, Turkiye VIII, Fitopatoloji Kongresi Bildirileri, 21–25 Eylül 1998, Ankara, Turkiye, 297–300.

Chang, M.C., Tanaka, J. (2002). FT-IR study for hydroxyapatite/collagen nanocomposite cross-linked by glutaraldehyde, *Biomaterials*, 23: 4811–4818.

Chen, X.M. (2002). Genetics of wheat resistance to stripe rust. Wheat rusts in China. Edited by Q.Li and S.M. Zeng. Chinese Agricultural Press, Beijing, China, 173–184.

Chen, X.M., and Line, R.F. (1995b). Gene number and heritability of wheat cultivars with durable, high-temperature, adult-plant resistance and race-specific resistance to *Puccinia striiformis*. *Phytopathology*, 85: 573–578.

Chen, X.M., and Line, R.F. (1992a). Identification of stripe rust resistance genes in wheat cultivars used to differentiate North American races of *Puccinia striiformis*. *Phytopathology*, 82: 1428-1434.

Chen, X.M., and Line, R.F. (1992b). Inheritance of stripe rust resistance in wheat cultivars used to differentiate races of *Puccinia striiformis* in North America. *Phytopathology*, 82: 633–637.

Chen, X.M., and Line, R.F. (1993). Inheritance of stripe rust resistance in wheat cultivars postulated to have resistance genes at *Yr3* and *Yr4* loci. *Phytopathology*, 83: 382–388.

Chen, X.M., and Line, R.F. (1993). Inheritance of stripe rust resistance in wheat cultivars postulated to have resistance genes at *Yr3* and *Yr4* loci. *Phytopathology*, 83: 382–388.

Chen, X.M., and Line, R.F. (1995a). Gene action in wheat cultivars for durable high-temperature adult-plant resistance and interactions with race-specific, seedling resistance to stripe rust caused by *Puccinia striiformis*. *Phytopathology*, 85: 567–572.

Chen, X.M., and Line, R.F. (1995b). Gene number and heritability of wheat cultivars with durable, high-temperature, adult-plant resistance and race-specific resistance to *Puccinia striiformis*. *Phytopathology*, 85: 573–578.

Chen, X.M., Jones, S.S., and Line, R.F. (1996). Chromosomal location of genes for resistance to *Puccinia striiformis* in seven wheat cultivars having resistance genes at *Yr3* and *Yr4* loci. *Phytopathology*, 86: 1228–1233.

Chen, X.M., Line, R.F., Shi, Z.X., and Leung, H. (1998a). Genetics of wheat resistance to stripe rust. *Proceedings of the 9th International Wheat Genetics Symposium*. 2–7 August 1998, University of Saskatchewan, Saskatoon, Sask. *Edited by* A.E. Slinkard. University Extension Press, University of Saskatchewan, Saskatoon, Sask., 3: 237–239.

Ci, X. Y., Gao, T. Y., Feng, J. and Guo, Z. Q. (1999). Fourier transform infrared characterization of human breast tissue: Implications for breast cancer diagnosis, *Applied Spectroscopy*, 53: 312-315.

CIMMYT, (2005). An Assessment of Race Ug99 in Kenya and Ethiopia and the Potential for Impact in Neighbouring Regions and beyond, Expert Panel on the Stem Rust Outbreak in Eastern

Colthup, N. B., Daly, L. H. and Wiberley, S. E. (1975). *Introduction to infrared and raman spectroscopy*, New York: Academic Press.

Dalvi A.G. I., Al-Rasheed R. and Javeed M. A. (2000). Studies on organic foulants in the seawater feed of reverse osmosis plants of SWCC. *Desalination*, 132: 217.

Desai R.M., Bhatia C.R. (1978). Nitrogen uptake and nitrogen harvest index in durum wheat cultivars varying in their grain protein concentration. *Euphytica*, 27: 561–566.

Dighton J, Mascarenhas M, Arbuckle-Keil G. (2001). Changing resources: assessment of leaf litter carbohydrate resource change at a microbial scale of resolution. *Soil Biology & Biochemistry*, 33: 1429.

Dubis E.N., Dubis A.T., Morzycki J.W. (1999). Comparative analysis of plant cuticular waxes using HATR FT-IR reflection technique. *Journal of Molecular Structure*, 511–512: 173–179.

Dubis E.N., Dubis A.T., Poplawski J. (2001). Determination of the aromatic compounds in plant cuticular waxes using FT-IR spectroscopy. *Journal of Molecular Structure*, 596: 83–88.

Dusunceli, F., Cetin, L., Albustan, S., Beniwal, S.P.S. (1998). Bazi uluslararası bugday hastalıkları dayanıklılık kaynaklarının Orta Anadolu'da sari pasa (*Puccinia striiformis* f.sp. *tritici*) reaksiyonlarının belirlenmesi, Türkiye VIII. Fitopatoloji Kongresi Bildirileri, 21–25 Eylül 1998, Ankara, Türkiye, 293–296.

Duveiller E., Singh R. P., Nicol J. M. (2007). The challenges of maintaining wheat productivity: pests, diseases, and potential epidemics. *Euphytica*, 157: 417–430.

FAOSTAT, (2009). (available at <http://faostat.fao.org/default.aspx>, last access date March, 2011).

Faris J. D., Xu S. S., Cai X., Friesen T. L., Jin Y. (2008). Molecular and cytogenetic characterization of a durum wheat- *Aegilops speltoides* chromosome translocation conferring resistance to stem rust. *Chromosome Research*, 16: 1097–1105.

Flor, H. H. (1942). Inheritance of pathogenicity in *Melampsora lini*. *Phytopathology*, 32: 653-669.

Freifelder, D. (1982). *Physical Chemistry. Applications to biochemistry and molecular biology*, Freeman, W. H. (Ed), New York.

Gocmen B., Albustan S., Kaya Z., Keskin S., Taskin V. (2003). Response of 150 F6 inbred durum wheat lines derived from Kunduru-1149 x Cham-1 cross to yellow rust (*Puccinia striiformis*), *Crop Protection* 22: 787–793.

Görgülü S.T., Dogan M., Severcan F.(2007). The characterization and differentiation of higher plants by FTIR spectroscopy. *Applied Spectroscopy*, 61 (3) : 310-316.

Haris, P. I. and Severcan F. (1999). FTIR spectroscopic characterization of protein structure in aqueous and non-aqueous media. *J. Molecular Catalysis B: Enzymatic*, 7: 207-221.

Helm, D., Labischinski, H., Schallehn, G., Naumann, D. (1991). Classification and identification of bacteria by Fourier-transform infrared spectroscopy. *J. Gen. Microbiol.*, 137: 69–79.

Hijwegen, T. (1963). Lignification, a possible mechanism of active resistance against pathogens. *Neth. J. Plant Pathol.*, 69: 314-317.

Hussain, M., Khan, M.A., Irsdhad, M., Hussain, M. (1999). Screening of wheat germplasm against leaf and stripe rust epidemics for the identification of resistant sources against these diseases. *Pak. J. Phytopathol.*, 11 (1): 93–99.

James, D.G., Clifford, B.C. (1983). *Cereal Diseases-Their Pathology and Control*. Wiley, New York, 300 pp.

Jamin N., Dumas P., Moncuit J., Fridman W., Teillaud J., Carr L.G. and Williams G.P. (1998). Highly resolved chemical imaging of living cells by using synchrotron infrared micrispectroscopy. *Appl. Biol. Sci.*, 95: 4837–4840.

Johnson R. (1984). A critical analysis of durable resistance. *Annu. Rev. Phytopathol.*, 22: 309–330.

Johnson, R. (1992). Past, present and future opportunities in breeding for disease resistance, with examples from wheat. *Euphytica*, 63: 3–22.

Joshi A.K., Mishra B., Prashar M., Tomar S.M.S., Singh R.P. (2008). Ug99 race of stem rust pathogen: challenges and current status of research to sustain wheat production in India. *Indian J Genet Plant Breed*, 68: 231–241.

Kacurakova M., Capek P., Sasinkova N., Wellner N., and Ebringerova A. (2000). FT-IR study of plant cell wall model compounds: pectic polysaccharides and hemicelluloses. *Carbohydr.Polym.*, 43: 195.

Khan, M.A., Yaqub, M., Nasir, M.A. (1998). Slow rusting response of wheat genotypes against *Puccinia recondita* f.sp. *tritici* in relation environmental conditions. *Pak. J. Phytopathol.*, 10 (2): 78–85.

Kimber, G., Feldman M. (1987). *Wild Wheat. An introduction*. Special Report 353, College of Agriculture, University of Missouri – Colombia, 129–131.

Kınacı, E., Kınacı, G. (1991). Orta Anadolu ve Gecit Kusagında bugday ve arpa hastalık paterni ve etkileri. VI. Türkiye Fitopatoloji Kongresi, 7–11 Ekim, İzmir, 133.

Kinder, R., Ziegler, C., Wessels, J.M. (1997). γ -Irradiation and UV-C light induced lipid peroxidation: A Fourier transform-infrared absorption spectroscopic study. *Int. J. Radiat. Biol.*, 71(5): 561-571.

Krimm S. and Bandekar J.(1986). Vibrational spectroscopy and conformation of peptides, polypeptides, and proteins. *Adv. Protein Chem.*, 38: 181–365.

Leonard K. J. and Szabo L.J. (2005). Stem rust of small grains and grasses caused by *Puccinia graminis*. *Molecular Plant Pathology*, 6 (2): 99-111.

Leonard K. J. (2001). Black stem rust biology and threat to wheat growers. Cereal Disease Lab., St. Paul, MN (Available at www.ars.usda.gov/Main/docs.htm?docid=10755&pf=1&cg_id=0., last access date March, 2011).

Line, R.F. and Chen, X.M. (1995). Successes in breeding for and managing durable resistance to wheat rusts. *Plant Dis.*, 79: 1254–1255.

Line, R.F., and Chen, X.M. (1996). Wheat and barley stripe rust in North America. In *Proceedings of the 9th European and Mediterranean*.

Line, R.F. and Qayoum, A. (1992). Virulence, aggressiveness, evolution, and distribution of races of *Puccinia striiformis* (the cause of stripe rust of wheat) in North America, 1968–87. *US Dep. Agric. Agric. Res. Serv. Tech. Bull.*, 1788.

Liyama K., Lam TBT., Stone B. A., (1994). Covalent Cross-Links in the Cell Wall. *Plant Physiol.*, 104(2): 315–320.

Liu, K.Z., Bose, R., Mantsch, H.H. (2002). Infrared spectroscopic study of diabetic platelets, *Vibrational Spectroscopy*, 28: 131–136.

Luig, N.H. and Watson, I.A. (1972). The role of wild and cultivated grasses in the hybridization of formae speciales of *Puccinia graminis*. Aust. J. Biol. Sci., 25: 335-342.

Lupton, F.G.H. and Macer, R.C.F. (1962). Inheritance of resistance to yellow rust (*Puccinia glumarum* Erikss., and Henn.) in seven varieties of wheat. Trans. Br. Mycol. Soc. 45: 21–45.

Lupton, F.G.H., Wilson, F.E., and Bingham, J. (1971). Breeding for non-race specific resistance to yellow rust and to mildew. 1970 Annual Report, Plant Breeding Institute Cambridge, UK.

Lyman, D. J. and Murray-Wijelath, J. (1999). Vascular graft healing: I. FTIR analysis of an implant model for studying the healing of a vascular graft. J. Biomed. Mater. Res., 48:172–186.

Mamluk, O.F. (1992). Durum wheat diseases in West Asia and North Africa (WANA). In: Rajaram, S., Saari, E.E., Hettel, G.P. (Eds.), Durum Wheats: Challenge and Opportunities. CIMMYT Wheat Special Reports No. 9, CIMMYT, Mexico, D.F., Mexico.

Manoharan, R., Baraga, J.J., Rava, R.P., Dasari, R.R., Fitzmaurice, M. and Feld, M.S. (1993). Biochemical analysis and mapping of atherosclerotic human artery using FTIR microspectroscopy. Atherosclerosis, 103:181-193.

Mantsch, H.H. (1984). Biological application of Fourier Transform Infrared Spectroscopy: A study of phase transitions in biomembranes. J. Mol. Structre, 113: 201-212.

Marsalis M. A., Goldberg N. P. (2011). Leaf, Stem and Stripe Rust Diseases of Wheat. (available at aces.nmsu.edu/pubs/_a/A-415.pdf, last access date March, 2011)

Mascarenhas M., Dighton J. and Arbuckle G. A. (2000). Characterization of Plant Carbohydrates and Changes in Leaf Carbohydrate Chemistry Due to Chemical and Enzymatic Degradation Measured by Microscopic ATR FT-IR Spectroscopy. *Appl. Spectrosc.*, 54: 681.

McIntosh, R. A., Wellings, C.R. and Park, R. F. (1995). *Wheat Rusts: an Atlas of Resistance Genes*. Dordrecht: Kluwer Academic Publishers.

McIntosh, R.A., Wellings C.R. and Park R.F. (1995b). *Wheat Rusts: An Atlas of Resistance Genes*. CSIRO Publications, Melbourne, Australia.

Melin, A., Perromat, A., and Deleris, G. (2000). Pharmacologic Application of Fourier Transform IR Spectroscopy: In vivo Toxicity of Carbon tetrachloride on rat liver. *Biopolymers (Biospectroscopy)*, 57: 160-168.

Mendelsohn, R. and Mantsch, H. H. (1986). Fourier transform infrared studies of lipid-protein interaction, *Progress in Protein-Lipid Interactions, Volume 2*, Elsevier Science Publishers, Netherlands, 103-147.

Merk S., Blume A., Riederer M. (1998). Phase behaviour and crystallinity of plant cuticular waxes studied by Fourier transform infrared spectroscopy. *Planta*, 204: 44–53.

Milus, E.A., and Line, R.F. (1986a). Number of genes controlling high-temperature adult-plant resistance to stripe rust in wheat. *Phytopathology*, 76: 93–96.

Milus, E.A., and Line, R.F. (1986b). Gene action for inheritance of durable, high-temperature, adult-plant resistance to stripe rust in wheat. *Phytopathology*, 76: 435–441.

Murray G.M., Brennan J.P. (2009). The current and potential costs from diseases of wheat in Australia. Australian Grains Research and Development Corporation report, 69.

Naumann A., Heine G., Rauber R. (2010). Efficient discrimination of oat and pea roots by cluster analysis of Fourier transform infrared (FTIR) spectra. *Field Crops Research*, 119: 78–84.

Parry, D.W. (1990). *Plant Pathology in Agriculture*. Cambridge University Press, Cambridge, 365pp.

Pasquini M., Sereni L., Casulli F., Siniscalco A., Mameli L., Gallo G., Prima G., Spina A., Liotta, C., Invernizzi C., Padovan S., Minoia C. (1998). Reaction of durum and bread wheats to some fungal diseases. *Inf. Agrari*, 54 (38): 63–73.

Poon, R., Richards, J., Clark, W. (1981). The relationship between plasma membrane lipid composition and physical–chemical properties: II. Effect of phospholipid fatty acid modulation on plasma membrane physical properties and enzymatic activities. *Biochim. Biophys. Acta.*, 649: 58–66.

Pretorius Z.A., Singh R.P., Wagoire W.W., Payne T.S. (2000). Detection of virulence to wheat stem rust resistance gene Sr31 in *Puccinia graminis*.f.sp. *tritici* in Uganda. *Plant Dis*, 84: 203.

Priestley, R.H. and Dodson, J.K. (1976). Physiological specialization of *Puccinia striiformis* to adult plants of winter wheat cultivars in the United Kingdom. In Proc. 4th Eur. Mediterr. Cereal Rusts Conf. 5–10 September 1976, Interlaken, Switzerland. 87–89.

Qayoum, A. and Line, R.F. (1985). High-temperature, adult-plant resistance to stripe rust of wheat. *Phytopathology*, 75: 1121– 1125.

Rana, F.R., Sultany, C.M. and Blazyk, J. (1990). Interactions between *Salmonella typhimurium* lipopolysaccharide and the antimicrobial peptide, magainin 2 amide. FEBS Letters, 261(2): 464-467.

Ride J., P. (1983). Cell walls and other structural barriers in defence. In JA Callow, ed, Biochemical Plant Pathology. John Wiley & Sons, Chichester, 215-223.

Rigas, B., Morgellot, S., Goldman, I.S., Wong, P.T.T. (1990). Human colorectal cancers display abnormal Fourier-transform infrared spectra. Proc. Nati. Acad. Sci., 87: 8140-8144.

Roelfs A.P., Singh R.P., and Saari E.E. (1992). Rusts diseases of wheat: concepts and methods of diseases management. CIMMYT, Mexico City.

Roelfs AP: Epidemiology of the cereal rusts in North America. Can J Plant Pathol 1989, 11:86-90.

Roelfs, A.P., (1986). Development and impact of regional cereal rust epidemics. In K. J. Leonard and W.E. Fry. eds. Plant Disease Epidemiology 1:129-150. MacMillan, New York.

Saari E.E. Prescott J.M. (1985). World distribution in relation to economic losses. In: Roelfs AP, Bushnell WR (eds) The cereal rusts, vol 2, diseases, distribution, epidemiology, and control. Academic Press, Orlando, Florida, 259–298.

Schultz, C. and Naumann D. (1991). In vivo study of the state of order of the membranes of Gram-negative bacteria by Fourier-transform infrared spectroscopy (FT-IR). FEBS Letters, 294: 43-46.

Severcan, F. (1997). Vitamin E decreases the order of the phospholipid model membranes in the gel phase: An FTIR study. Bioscience Reports, 17: 231-235.

Severcan, F., Gorgulu, G., Gorgulu, S.T., Guray, T. (2005). Rapid monitoring of diabetes-induced lipid peroxidation by Fourier transform infrared spectroscopy: Evidence from rat liver microsomal membranes. *Anal. Biochem.*, 339: 36–40.

Severcan, F., Kaptan, N., Turan, B. (2003). Fourier transform infrared spectroscopic studies of diabetic rat heart crude membranes. *Spectroscopy*, 17: 569–577.

Severcan, F., Toyran, N., Kaptan, N. and Turan, B. (2000). Fourier transform infrared study of diabetes on rat liver and heart tissues in the C-H region. *Talanta*, 53: 55-59.

Simmonds, N.W., and Rajaram S. (Eds.), (1988). *Breeding Strategies for Resistance to the Rusts of Wheat*. CIMMYT, Mexico D.F., Mexico. 151 pp.

Singh R.P., Hodson D.P., Huerta-Espino J., and Yue J. (2008). Will stem rust destroy the world's wheat crop? *Adv Agron.*, 98:271–309.

Singh R.P., Huerta Espino J., Manilal H.M. (2005). Genetics and breeding for durable resistance to leaf and stripe rusts in wheat. *Turk J Agric. For.*, 29:121-127.

Singh R.P., Huerta-Espino J., Roelfs A.P. (2002). The wheat rusts. In: Curtis BC, Rajaram S, Go'mez Macpherson H (eds) *Bread wheat: improvement and production*, plant production and protection series no. 30, FAO, Rome, 227–249.

Singh R.P., Trethowan R. (2007). Breeding spring bread wheat for irrigated and rainfed production systems of the developing world. In: Kang M, Priyadarshan PM (eds) *Breeding major food staples*. Blackwell, Iowa, 109–140.

Smith, B. C. (1999). *Infrared spectral Interpretation* CRC Press LLC. Printed in USA.

Smith, G.C.M., and Jackson, S.P. (1999). The DNA dependent protein kinase. *Genes Dev.*, 13: 916-934.

Stakman, E.C., Stewart, D.M. and Loegering, W.Q. (1962). Identification of physiologic races of *Puccinia graminis* var. *tritici*. U.S.Dept. Agric., Agric. Res. Serv. Publ. E 617.

Steele, D. (1971). *The Interpretation of Vibrational Spectra*, William Clowes & Sons Lim., Great Britain.

Strange R. N., and Scott P. R. (2005). Plant Disease: A Threat to Global Food Security, *Annu. Rev. Phytopathol.*, 43:83–116.

Stuart, B. (1997). *Biological Applications of Infrared Spectroscopy*. John Wiley and Sons, Ltd., England.

Szalontai, B., Nishiyama, Y., Gombos, Z., and Murata, N. (2000). Membrane dynamics as seen by Fourier Transform Infrared Spectroscopy in a cyanobacterium, *synechocystis* PCC 6803. The effects of lipid unsaturation and the protein-to-lipid ratio. *Biochim.Biophys. Acta.*, 1509; 409-419.

Takahashi, H., French, S. M., and Wong, P. T. T. (1991). Alterations in hepatic lipids and proteins by Chronic ethanol Intake: A high pressure fourier transform Infrared spectroscopic study on alcoholic liver disease in the rat alcohol. *Clin. Exp. Res.*, 15(2): 219-223.

Toyran N. and Severcan F. (2003). Competitive effect of vitamin D(2) and Ca⁽²⁺⁾ on phospholipid model membranes: an FTIR study. *Chem. Phys. Lipids*, 123 (2):165-176.

Toyran, N., Zorlu, F., Dönmez, G., Öge, K., Severcan, F. (2004). Chronic hypoperfusion alters the content and structure of proteins and lipids of rat brain homogenates: A Fourier transform infrared spectroscopy study. *Eur. Biophys. J.*, 33: 549–554.

Toyran, N., Lasch, P., Naumann, D., Turan, B., Severcan, F. (2006). Early alterations in myocardia and vessels of the diabetic rat heart: an FTIR microspectroscopic study. *Biochem J.*, 397(3):427-436.

Umemura J., Cameron G., and Mantsch H. H. (1980). A Fourier transform infrared spectroscopic study of the molecular interaction of cholesterol with 1,2-dipalmitoyl-sn-glycero-3-phosphocholine. *Biochim Biophys Acta.*, 602(1):32–44.

Vance C. P., Kirk T. K., Sherwood R. T. (1980). Lignification as a Mechanism of Disease Resistance. *Ann. Rev. of Phytopathol.*, 18: 259-288.

Web site of Cereal Disease Encyclopaedia, (available at http://www.hgca.com/minisite_manager.output/3625/3625/Cereal%20Disease%20Encyclopedia/Diseases/Yellow%20%28Stripe%29%20Rust.aspx?minisiteId=26, last access date April, 2011).

Web site of Food and Agricultural Organization of the United Nations (FAO) (available at <http://faostat.fao.org/site/567/DesktopDefault.aspx?PageID=567#ancor>, last access date March, 2011).

Web site of Food and Agricultural Organization of the United Nations (FAO) (available at <ftp://ftp.fao.org/docrep/fao/011/i0378e/i0378e.pdf>, last access date August, 2011).

Web site of International Maize and Wheat Improvement Center (available online at http://www.globalrust.org/db/attachments/resources/737/10/BGRI_2009_proceedings_cimmyt_isbn.pdf, last access date: April 2011).

Web site of Molecular Expressions. (available at <http://micro.magnet.fsu.edu/primer/java/electromagnetic/index.html>, last access date September, 2011)

Web site of United States Department of Agriculture (USDA). (available at <http://www.fas.usda.gov/psdonline/psdReport.aspx?hidReportRetrievalName=World+Wheat+Production%2c+Consumption%2c+and+Stocks++++&hidReportRetrievalID=750&hidReportRetrievalTemplateID=7>, last access date March,2011).

Web site of United States Department of Agriculture (USDA). (available at <http://www.pecad.fas.usda.gov/highlights/2010/11/global%20durum/>, last access date march, 2011).

Web site of United States Department of Agriculture (USDA). (available at http://www.fas.usda.gov/pecad2/highlights/2003/11/durum%202003/Turkey_and_Syria.htm, last access date June, 2011).

Wong, P.T.T., Wong, R.K., Caputo, T.A., Godwin, T.A., Rigas, B. (1991). Infrared spectroscopy of exfoliated human cervical cells: Evidence of extensive structural changes during carcinogenesis. *Proc. Nati. Acad. Sci.*, 88: 10988-10992.

Yang J. and Yen H. E. (2002). Early Salt Stress Effects on the Changes in Chemical Composition in Leaves of Ice Plant and Arabidopsis. A Fourier Transform Infrared Spectroscopy Study. *Plant Physiol. Preview*, 130: 1032.

Yeagle P., L. (1989). Lipid regulation of cell membrane structure and function. *The FASEB Journal*, 3: 1833-1842.

Yono, K., Ohoshima, S., Shimuzu, Y., Moriguchi, T. and Katayama, H. (1996). Evaluation of glycogen level in human lung carcinoma tissues by an infrared spectroscopic method. *Cancer Letters*, 110:29-34.

Zadoks, J.C., (1963). Epidemiology of wheat rusts in Europe. *FAO Plant Protection Bull.* 13: 97–108.

Zhang P., McIntosh R., A., Hoxha S., Dong C. (2009). Wheat stripe rust resistance genes *Yr5* and *Yr7* are allelic. *Theor Appl Genet*, 120:25–29.

Zimmermann B. (2010). Characterization of Pollen by Vibrational Spectroscopy. *Applied Spectroscopy*, 64(12): 1364-1373.